



# Free radical synthesis of cross-linking gelatin base poly NVP/acrylic acid hydrogel and nanoclay hydrogel as cephalixin drug deliver

Amir Hajikarimi<sup>1</sup> · Mohammad Sadeghi<sup>1</sup>

Received: 28 November 2018 / Accepted: 29 January 2020 / Published online: 11 February 2020  
© The Polymer Society, Taipei 2020

## Abstract

In this research, we presented the synthesis of cross-linking poly N-vinyl pyrrolidone /acrylic acid hydrogel and nanoclay hydrogel based on gelatin which named gelatin-g-NVP-AA, gelatin-g-NVP-AA/MMT and used them as cephalixin drug delivery. These hydrogels were fully characterized by FTIR, SEM, TEM, XRD, TGA, DSC. Also, the effect of difference saline solution, temperature, the percentage of nanoclay and time were investigated. In addition, because of pH sensitivity of hydrogels, the swelling, drug loading and drug releasing were studied in different pHs, distilled water and buffers to determine the best condition for each situation which resulted illustrated the universal buffer in pH 8 was the least interaction with hydrogels and had maximum drug loading and releasing in this condition. Antibacterial activities of hydrogels were examined against the *S. aureus* and the *E. coli* and showed an interesting result for the loaded drug on gelatin-g-NVP-AA/MMT.

**Keywords** Gelatin · Nano composites · Hydrogels · Antibacterial activities · Drug loading

## Introduction

The term “Polymer hydrogels,” is used to introduce materials which have mention as three-dimensional polymeric networks that are formed with highly hydrophilic monomers to build high-molecular-weight polymeric network that are able to imbibe huge quantity of water or aqueous solution or biological fluids by covalent crosslinking, hydrogen bond or electrostatic in their construction to balance without network dissolution [1–4]. The responsibility of high water absorption by hydrogel networks carry out by the existence narrow vessel areas in the network and hydrophilic nature of functional groups on the polymeric structure that can be classified as neutral, ionic such as  $-\text{CO}_2\text{Na}$ ,  $-\text{CO}_2\text{H}$ ,  $-\text{SO}_3\text{H}$ ,  $-\text{CO}_2\text{NH}_3$ , or on-ionic  $-\text{OH}$ ,  $-\text{CONH}-$ ,  $-\text{CHO}$ ,  $-\text{O}-$ ,  $-\text{NH}_2$  and osmotic pressure in different parts of hydrogel networks [5–7].

Hydrogels have significantly slight toxicity, inflammatory responses and tissue damaging and excellent biodegradability and biocompatibility which show reversible responses to stimuli-responsive such as temperature, pH, magnetic field,

electric field and ionic strength of solution with biological molecules that make them as intelligent or smart hydrogels [8–10].

Since these significant properties hydrogel are useful in the different range of applications including pharmaceuticals, drug delivery, biotechnology, tissue engineering, agriculture, food processing, wastewater purification, and biosensors and bioactuators in biomicroelectro mechanical systems (BioMEMS) [11–18].

Many research groups recently have focused on improving hydrogels to enrich their swell or de-swell in water and to keep the swollen state, gel strength that can be done by the synthesis of cross-linking of hydrophilic polymers-monomers hydrogel either by a chemical method or by radiation method [6, 19, 20].

Hydrogels based on Poly vinylpyrrolidone (PVP) are a well-known biologically and eco-friendly that have excellent solubility in water, absorbency, mucoadhesive and biocompatibility which have been utilized to treat wound as the local dressings in burning, skin’s ulceration and postoperative and controlled for releasing in drug delivery system [21–24]. However, because of low mechanical properties in hydrogels of PVP, they have limitation for using in some applications [25].

Copolymerization N-vinyl pyrrolidone (NVP) via acrylic acid (AA), methacrylates and other vinyl monomers have been investigated to receive PVP-PAA crosslinked complexes that enhance the mechanical properties and its biocompatibility and water uptake [25–29]. Because of the pH and electrically sensitive of

✉ Mohammad Sadeghi  
m-sadeghi@iau-arak.ac.ir

<sup>1</sup> Department of chemistry, Arak branch, Islamic Azad University, Arak, Iran

acrylic acid due to having carboxylic acid groups, PVP-PAA hydrogels have been applied in pH-controlled loading and releasing rate for drug delivery and preparation of mucoadhesive microspheres and polymer-ceramic composites [26–31].

However, high costly production and weak natural mechanical strength of hydrogels have unfortunately limited their practical applications [32]. So, researchers attempt to reinforce the hydrogels conformation to achieve nanocomposite hydrogels by improving chemical, Physical and mechanical properties by using nanoparticles or nanostructures [33–36].

For preparation nanocomposites hydrogels have been used clays nanoparticles like laponite [37, 38], hydrotalcite [39], bentonite [40], and Na-montmorillonite [41–43] which develop biomedical applications in drug delivery systems, contact lenses and in-vitro [44] and in-vivo [45] wound dressing systems by changing their excellent mechanical properties, high water swelling, good biocompatibility and reducing effectively cost of hydrogels [46–48].

Cephalexin (Ce) is an antibiotic  $\beta$ -lactam that can use against a number of bacterial infections. It is significantly useful for killing both gram-positive and some gram-negative bacteria by disturbing the cell wall growing in the bacteria [49, 50]. It is very critical for the drug releasing along the intestine for the treatment of microbial infections [51, 52]. Some literature has been reported the investigation of synthesis and biological activities of nano antibiotic  $\beta$ -lactam [53, 54] and copolymerization them that have tested again bacteria [55, 56].

## Experimental section

### General

#### Chemical reagents

Gelatin (average Mw = 190000–220000) was prepared by Aldrich (USA). Acrylic acid (AcA; MW = 72.06 g mol<sup>-1</sup>, d = 1.06 g mL<sup>-1</sup>, purity >99% from Fluka) was utilized as a monomer after vacuum distillation. N-Vinyl pyrrolidone was purchased from Merck and used upon arrival. N, N-Methylene bisacrylamide (MBA) from Merck as a crosslinker, Montmorillonite (MMT) from Aldrich and ammonium persulfate (APS) from Fluka as a thermal initiator were purchased and used immediately. The cephalexin with purity >99% was purchased from Farabi pharmaceutical industry. The bacteria, *S. aureus* (ATCC-6538) and *E. coli* (ATCC-25922) were kindly provided by microbiology laboratory of Islamic Azad University, Arak, Iran.

#### Instruments

Fourier transform infrared spectroscopy (FT-IR) analysis of the samples was taken on a Shimadzu FT-IR 8300

spectrophotometer. The phase formation and crystallographic state of nanoparticles were determined by PW 17c phelix X-ray diffractometer with Cu Ka radiation ( $\lambda = 1.5418$ ).

The size and morphology of the nanoparticles were observed using a LEO 912AB transmission electron microscope (TEM) with an acceleration voltage 100 kV in 31X-680 KX. The nanoparticles were thoroughly dispersed in water by ultrasonication and placing a drop of solution on the carbon coated copper grid. Field Emission Scanning Electron Microscopy (FE-SEM) images were obtained on TE-SCAN, MIRA III. The hydrodynamic size of the particle was measured by dynamic light scattering (DLS) techniques, using a HORIBA-SZ-100 particle size analyzer. Thermogravimetric analysis (TGA) and differential scanning calorimetric (DSC) were carried out using Q600 with Ar carrier gas and the rate of temperature change of 20 °C min<sup>-1</sup>. BET analysis was used to determine surface area by BELSORP MINI II and degassing devise was BELPREP VAC II. A Shimadzu UV-visible Agilent-8541 spectrophotometer was used for recording absorption spectra in solution. Photolyses were performed using a low-pressure mercury lamp with a transmission maximum at  $\lambda = 254$  nm (85% transmission) and transmitted light from 254 to 579 nm (15% transmission). Drug releasing was performed by HPLC using the SGX, C18 column.

### Synthesis of cross-link gelatin-g-PVP-AA hydrogel

For the synthesis of cross-link gelatin-g-PVP-AA hydrogel, 25 ml of distilled water was poured into a beaker that equipped with a mechanical stirrer and placed in a constant-temperature bath at 80 °C. Then, a certain amount of gelatin (0.3 g) was added to the beaker and used the mechanical stirrer to dissolve completely. After gelatin dissolved and homogenized, the monomers, AA (6 mL), NVP (2.5 mL) and the MBA as crosslinker (0.06 M) were added simultaneously and kept the reaction mixture was stirred for 15 min. Then the ammonium persulfate (APS, 0.05 M) as a radical initiator was added to the mixture and copolymerization was observed after around 40 min. After cooling the reactor, 1 N sodium hydroxide was added drop wise to the reaction mixture and kept for 1 h for partly neutralization by treating with the carboxylic groups of the excess of acrylic acid. For removing the water, the hydrogel was poured to 100 mL ethanol for 3 h, and then the dried hydrogel was cut in small pieces and kept in the oven for 24 h at room temperature to completely remove water. Then, the obtained hydrogel was ground and separated with the graded sieve between particles of 40 to 60 meshes (250–350  $\mu$ m) and kept away from light and moisture for further research.

## Synthesis of cross-link gelatin-g-NVP-AA/MMT nanocomposite hydrogel

For the synthesis of nano-clay cross-link gelatin-g-NVP-AA/MMT hydrogel had been used as the same procedure that explains the synthesis of cross-link NVP-AA hydrogel instead of sodium montmorillonite (Na-MMT) was added before the adding MBA. For this aim, the monomers, AA (4 mL) and NVP (2 mL) were added to the dissolved gelatin (0.3 g) in 25 ml of distilled into a beaker that equipped with mechanical stirrer and placed in a constant-temperature bath at 80 °C. Then, a certain amount of Na-MMT (0.008 M) was added to the reaction mixture and stirred for 30 min. After that, the MBA as crosslinker (0.10 M) were added simultaneously and kept the reaction mixture was stirred for 15 min. Then the APS (0.05 M) as a radical initiator was added to the mixture and copolymerization started and completed after around 40 min. After cooling the reactor, 1 N sodium hydroxide was added drop wise to the reaction mixture and kept for 1 h for partly neutralization by treating with the carboxylic groups of the excess of acrylic acid. For removing the water, the hydrogel was poured to 100 mL ethanol for 3 h, and then the dried hydrogel was cut in small pieces and kept in the oven for 24 h at room temperature to completely remove water. Then, the obtained hydrogel was ground and separated with the graded sieve between particles of 40 to 60 meshes (250–350 μm) and kept away from light and moisture for further research.

### Concentration measurement method

Due to the absorption wavelength of Cephalexin in the UV region, the UV-visible spectrophotometer and HPLC chromatography were used to measure the concentrations. To do this, a corresponding standard curve was prepared and by using this curve, the conversion rate of absorption to the material concentration in a given volume is easily accomplished [57].

### Water swelling measurement

An appropriately weighed samples ( $0.1 \pm 0.0001$  g) of the powdered gelatin-g-PVP-AA and gelatin-g-PVP-AA/MMT nanocomposite hydrogels as superabsorbent were tested swelling capacity by “tea bag” method with average particle sizes between 40 to 60 mesh (250–350 μm) by immersing in 200 ml distilled water for 3 h. The equilibrium swelling (ES) capacity was calculated twice at room temperature by the following formula (1):

$$ES(g/g) = \frac{W_2 - W_1}{W_1} \quad (1)$$

Where in this formula  $W_1$  and  $W_2$  are the weights of dry and swollen gel, respectively.  $E_s$  was calculated at 450 and

557 (g/g) for gelatin-g-PVP-AA and gelatin-g-PVP-AA/MMT nanocomposite hydrogels, respectively.

### Measuring the amount of hydrogel swelling in different salt solutions

To measure the rate of swelling or absorption of synthetic the gelatin-g-PVP-AA and gelatin-g-NVP-AA/MMT nanocomposite hydrogels, 1.0 g of compounds was immersed in different 0.1 M salt solution such as LiCl, NaCl, KCl, RbCl, CsCl, and calculated the equilibrium swelling rate. In addition, the hydrogel and nanocomposite hydrogel balance equilibrium capacity were also measured in concentrations of 0.01, 0.20, 0.05, 0.1, 0.15, 0.20 and 0.25 M of NaCl,  $CaCl_2$  and  $AlCl_3$ .

### Study of swelling kinetic

To study the Hydrogel swelling kinetics, their swelling rates are measured with different particle sizes. For this purpose, with special sieves, particle size of 100–250, 250–400, and 550–400 were separated and placed inside the tea bag and it was immersed in containing 200 ml of distilled water beaker and measured the amount of water absorption of hydrogel and nanocomposite hydrogel at different times (1 to 120 min) after extraction of excess water.

### Study of hydrogels swelling sensitivity to pH

To determine the sensitivity of the synthesized hydrogels to the pH, the swelling was measured in buffers at pH 1 to 12. Buffer solutions were prepared and 0.1 g of hydrogels was kept for 3 h in the beaker containing 200 ml buffer solution and was obtained the amount of hydrogels' swelling in buffer solutions.

### Drug loading of cephalexin on hydrogels

The drug solution was prepared at a concentration of 200 ppm and then 0.5 g of synthesized gelatin-g-NVP-AA and gelatin-g-NVP-AA/MMT nanocomposite hydrogels were added to the drug solution and for two days. The hydrogels were placed at a constant temperature to absorb the drug by hydrogels. The specimens were then filtered and washed with a portion of distilled water to remove the adherent drug completely from the hydrogels. The volume of the filtrate was measured and one sample was taken to obtain the total amount of drug loaded. The loaded hydrogels were dried by vacuum oven at 40 °C and screened by sieve labeled with a mesh of 40 to 60 (250 to 350 μm) and these loaded hydrogels were used to examine the release of the drug [57].

### Study of the amount loading drug in different salt solutions

A solution of NaCl, CaCl<sub>2</sub> and AlCl<sub>3</sub> (0.01 M) were prepared and then the drug was added at a specific concentration to each salt solution. Then, 0.5 g of synthesized gelatin-g-PVP-AA and gelatin-g-PVP-AA/MMT nanocomposite hydrogels were added to a solution containing drug and salt for two days and were placed at a constant temperature to absorb the drug. After that, the samples in salt solutions were filtered and washed with a portion of distilled water to rinse the drug completely from the surface of the hydrogels. A volume of the filtrate was taken to obtain the total amount of loaded drug in saline solutions and measured with UV spectroscopy.

### Investigating the nanoclay effect on the amount of drug loading

The amount of 1.0 g of nanocomposite hydrogel containing various amounts of nanoclay (0.008–0.02 g) was added in 50 ml of the drug solution with certain concentration and kept at a constant temperature for a certain time. Then loaded drug hydrogels were filtered and the filtrate was used to calculate the total amount of drug loaded by UV spectroscopy.

### Effect of duration time on the amount of drug loading

The amount of 0.1 g of gelatin-g-NVP-AA and gelatin-g-NVP-AA/MMT nanocomposite hydrogels were added in 50 ml of a solution of the drug at a specified concentration and fixed at a constant temperature for a specified period of time, then, after a specified period, the loaded hydrogels were filtered. Then, the absorbance of the filtrate was measured to determine the total amount of drug loaded by UV spectroscopy. This method has been repeated over time [57].

### Study of the drug releasing in different buffers

To select the appropriate buffer for the drug releasing, three buffers containing salt buffers (Table 1), universal buffer (Britton–Robinson buffer (0.04 M H<sub>3</sub>BO<sub>3</sub>, 0.04 M H<sub>3</sub>PO<sub>4</sub>

and 0.04 M CH<sub>3</sub>CO<sub>2</sub>H)) [58] and stock buffer pH 13 (NaOH), pH 1 (HCl)) solutions were prepared and the drug interactions with these buffers were investigated to select the buffer with the least interaction with the drug [57].

### Investigating the temperature effect on the amount of drug releasing

According to the previous method, for the determination of temperature in the drug releasing, a certain amount of drug loaded on gelatin-g-NVP-AA and gelatin-g-NVP-AA/MMT nanocomposite hydrogels (0.03 g) were added to the 100 ml beaker containing 100 ml of buffer solution with a certain pH at three different temperatures (25, 35 and 43 °C) at the certain time. The release concentration of the drug was measured at each temperature by UV spectroscopy.

### Time effect on drug releasing

The amount of 0.1 g of gelatin-g-NVP-AA and gelatin-g-NVP-AA/MMT nanocomposite hydrogels were added in 50 ml of a solution of the drug at a specified concentration and fixed at a constant temperature for a specified period of time, then, after a specified period, the loaded hydrogels were filtered. Then, the absorbance of the filtrate was measured to determine the total amount of drug releasing by UV spectroscopy. This method has been repeated over time [57].

### Controlled the drug releasing test in different pHs

In this series of experiments, a certain amount of drug loaded on gelatin-g-NVP-AA and gelatin-g-NVP-AA/MMT nanocomposite hydrogels (0.2 g) were added to the 100 ml beaker containing 100 ml of a buffer solution with a certain pH at 37 °C. By permeation, the buffer solution into the hydrogels and swelling it, the drug is released gradually from the hydrogels, and the concentration of drug increased in the buffer solution. To measure the concentration of the drug during its release into a buffer solution, at certain time intervals, 3.5 ml of solution was taken from the sample and absorbance was measured. In order to avoid changing the system concentration, this volume of the

**Table 1** Preparation of salt buffer solution

Materials required for 1000 cc salt buffer						
pH				pH		
1	HCl = 8.3 cc	–		8	Na <sub>2</sub> HPO <sub>4</sub> = 12.91 g	NaH <sub>2</sub> PO <sub>4</sub> = 0.88 g
3	NaH <sub>2</sub> PO <sub>4</sub> = 5.7 g	H <sub>3</sub> PO <sub>4</sub> = 0.34 cc		10	Na <sub>2</sub> CO <sub>3</sub> = 1.39 g	NaHCO <sub>3</sub> = 2.38 g
5	CH <sub>3</sub> COONa = 3.65 g	CH <sub>3</sub> COOH = 0.86 cc		12	NaOH = 4 g	–
7	Na <sub>2</sub> HPO <sub>4</sub> = 5.79 g	NaH <sub>2</sub> PO <sub>4</sub> = 3.98 g				



buffer solution was returned to the system in the same conditions to maintain the volume constant during the test. This test was done at pH 1, 3, 5, 7, 8, 10 and 12 to evaluate the drug's release at different pHs. Also, the drug releasing tests were performed in a similar manner of the human body in a solution with pH = 1.6 (stomach condition) and a solution with pH = 7.4 (intestinal condition) at 37 °C and its release rate was measured by UV spectroscopy and HPLC [3].

### Antibacterial test

The synthesized hydrogels were used by using the agar diffusion method to determine to the antibacterial potential activity against both the gram-negative *Escherichia coli* (ATCC-25922) and the gram-positive *Staphylococcus aureus* (ATCC-6538). For this purpose, a part of Gelatin-g-NVP-AA, Gelatin-g-NVP-AA/MMT and Gelatin-g-NVP-AA/MMT/Ce hydrogels were prepared in distilled water with 1 ppm concentration and loaded on nutrient agar plates which contained the grew bacteria and sterilized by autoclaving for 1 h at 120 °C. The inhibition zones were calculated by averaging the diameters (mm) in three directions after 24 h incubation of the inoculated plates at 37 °C.

## Results and discussion

### Synthesis and characterization

#### Synthesis of hydrogels, nanocomposite hydrogel and their drug loading

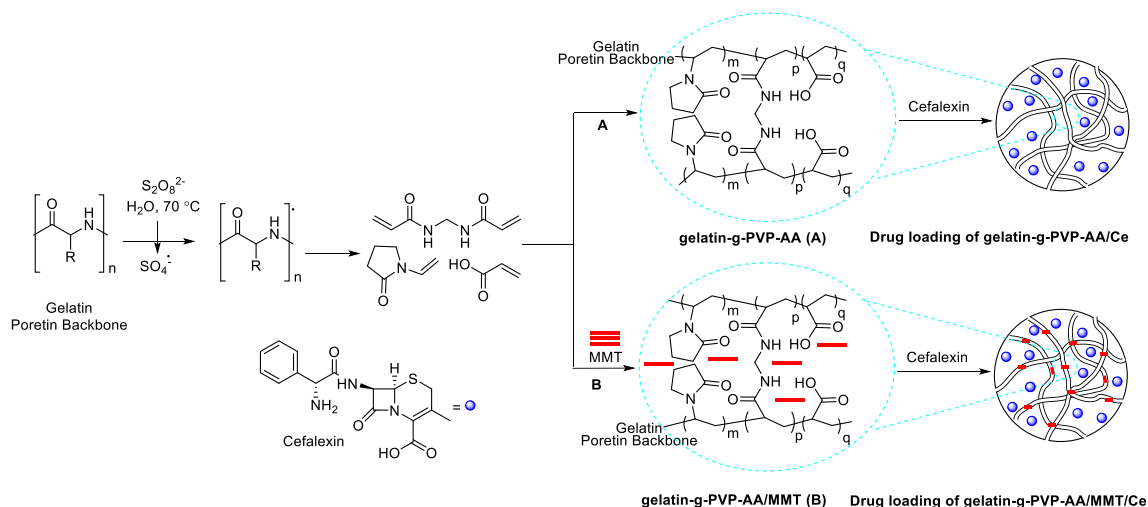
The synthesis of the crosslinking and graft polymerization process gelatin-g-NVP-AA (A), gelatin-g-NVP-AA/MMT (B) were shown in scheme 1. In this process, gelatin was used as a protein backbone to graft and copolymerize the hydrogel and

nanocomposite hydrogel. Totally, because of high molecular weight in polymer structure of proteins, gelatin has low solubility in aqueous solution. But grafting with copolymerization in their structure the solubility gets improved in the aqueous solution. For the copolymerization NVP and AA, monomers were used in the solution of gelatin and the NMB monomer was used as the cross-linking agent. The copolymerization started at 70 °C in a constant-temperature bath when APS was decomposed to make radical initiator by abstracting hydrogen from functional groups such as COOH, OH in a side chain [59]. After completing the reaction for the removing the excess of acrylic acid and naturalizing carboxylic groups, 1 N NaOH was poured in the reaction mixture. After naturalizing, the reaction mixture was poured in EtOH to remove water and after that, the resulting wet product kept in the oven to dry completely. The resulting product was called gelatin-g-NVP-AA that shown in scheme 1 which obtained from pathway A. As the same procedure for the synthesis of gelatin-g-NVP-AA/MMT, the NaMMT was added to the crude mixture before adding NMB which shown in pathway B in Scheme 1. After preparation of gelatin-g-NVP-AA (A) and gelatin-g-NVP-AA/MMT (B), the cephalexin was loaded. For this goal, 1 g of gelatin-g-PVP-AA and gelatin-g-NVP-AA/MMT nanocomposite hydrogels were poured into a 500 and 90 ppm solution of drug for 2 days and after that the drug-loaded hydrogel and nanocomposite hydrogel were filtered and washed that schematic form of a 3D network of each produces gelatin-g-NVP-AA/Ce and gelatin-g-NVP-AA/MMT/Ce were shown in scheme 1.

#### Characterization of hydrogel and nanocomposite hydrogel

##### FTIR analysis of hydrogel and nanocomposite hydrogel

For the confirmation of the network structure of the prepared hydrogel and nanocomposite hydrogel, FTIR was



**Scheme 1** Schematic diagram for synthesis of gelatin-g-NVP-AA and gelatin-g-NVP-AA/MMT and drug loading

used which is the unique technique to confirm original functional groups by detecting the shifting a bond in the spectrum. For comparison spectra, the combination of NVP-AA (A), NVP-AA/MMT (B), pure Cephalexin (C), hydrogel NVP-AA/Ce and nanocomposite hydrogel NVP-AA/MMT/Ce after loading with Cephalexin (D and E) spectra were shown in Fig. 1. As shown in Fig. 1, the spectra A-E clearly showed a broadband at the 3000–3500  $\text{cm}^{-1}$  which presented OH group in carboxylic acid that existed in PVP-AA, PVP-AA/MMT and Cephalexin structure. Also, asymmetric and symmetric stretching peaks of methyl and methylene groups exhibited about at 2920 and 2780  $\text{cm}^{-1}$ , respectively in the spectrum A-E. The spectrum of A represented three main peaks at the area of 1470, 1545 and 1712  $\text{cm}^{-1}$  which related to stretching C=O symmetric and asymmetric stretch of the carboxylate anion onto acrylic acid monomers and stretching COOH in non-ionized form, respectively [9]. Furthermore, the spectrum of B represented the absorption peaks at 1747  $\text{cm}^{-1}$  and 1050  $\text{cm}^{-1}$  that attributed to the ester groups formed during graft copolymerization and Si-O stretching onto MMT skeleton. As already mentioned, the carboxylic groups of the grafted AA-co-NVP can react with the OH groups on the silica gel surface [43]. The replacement of hydroxyl groups on the surface of montmorillonite by carboxylate anions results in the ester formation. The FTIR spectrum of Cephalexin (C) showed a sharp peak at the area of 1750 that related to stretching C=O in the  $\beta$ -lactam ring [60]. This peak could be able to see in (D) and (E) spectra that confirmed the Cephalexin had loaded on NVP-AA and NVP-AA/MMT hydrogels.

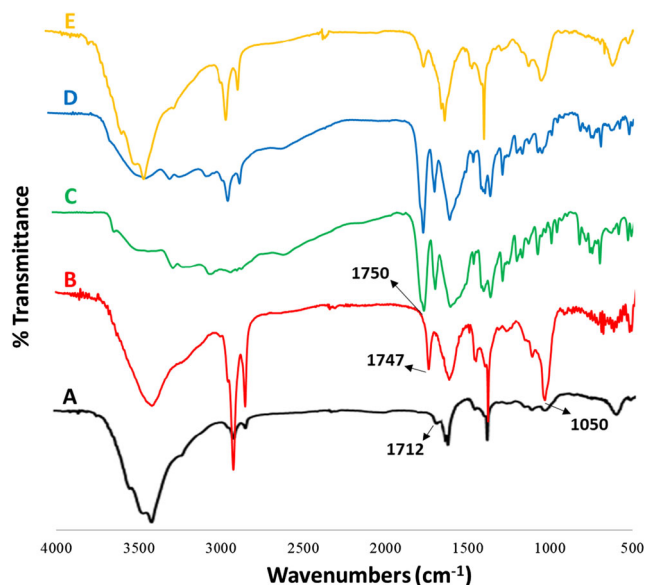


**Fig. 1** FTIR spectra of gelatin-g-NVP-AA (a), gelatin-g-NVP-AA/MMT (b), Cephalexin (c), gelatin-g-NVP-AA/Ce (d) and gelatin-g-NVP-AA/MMT/Ce (e)

## TGA and DSC analysis of gelatin-g-NVP-AA and gelatin-g-NVP-AA/MMT hydrogels

For thermal stability of gelatin-g-NVP-AA and gelatin-g-NVP-AA/MMT hydrogels, TGA analysis was used and the TGA curves of them were shown in Fig. 2. In TGA thermogram could detect four three losing weigh in different temperatures for both compounds. In the first step of losing weight corresponded to the evaporating of water from the surface and internal of molecules which were 2.93 and 5.87% in 149 °C for hydrogels and nanocomposite hydrogel, respectively. By increasing the temperature, the degradation of side chain started and the data showed the degradation for gelatin-g-NVP-AA/MMT hydrogel was 26.37% in 332 °C which this portion in 335 °C for gelatin-g-NVP-AA hydrogel was 33.91%. In 335 °C TGA thermogram showed a big gap between the gelatin-g-NVP-AA and gelatin-g-NVP-AA/MMT hydrogels losing weight which was 78.3 and 52.1% for hydrogels and nanocomposite hydrogel, respectively that represented to the degradation of the polymer backbone. In totally, the results showed that nanocomposite hydrogel was more stable than hydrogel and both cross-link copolymers were stable in the room temperature which was useful for the medicine release.

The differential scanning calorimetric (DSC) analysis is a thermo analytical technique which illustrates the change in the amount of heat required to increase the temperature of a sample. DSC is used widely for examining polymeric materials to determine their thermal transitions. So, this technique was used for gelatin-g-NVP-AA and gelatin-g-NVP-AA/MMT hydrogels to show the amount heat needed to increase the temperature and changes in their structures. According to Fig. 3, both gelatin-g-NVP-AA and gelatin-g-NVP-AA/MMT hydrogels thermogram showed the two minimum which was endothermic peaks. The gelatin-g-PVP-AA thermogram showed two peaks in 238.7 and 423.8 °C that the first peak resulted of melting of gelatin-g-NVP-AA hydrogel with  $\Delta H$  7.83  $\text{J g}^{-1}$  and the second peak related to amount heat for

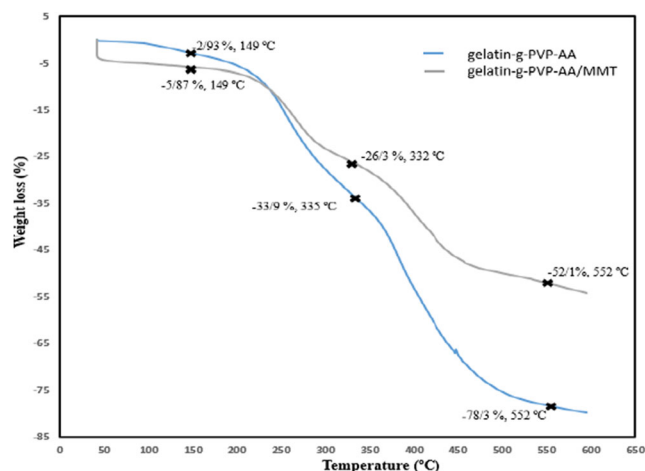
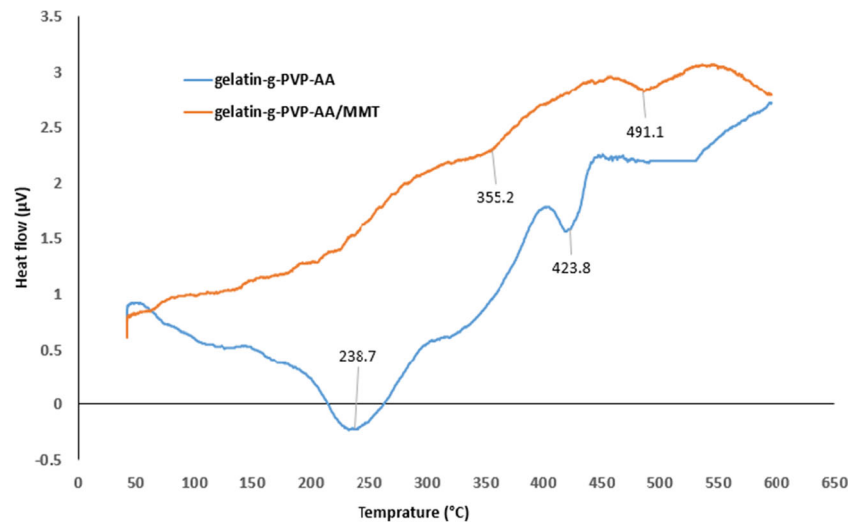


**Fig. 2** TGA curves of gelatin-g-PVP-AA and gelatin-g-PVP-AA/MMT hydrogels

**Fig. 3** DSC thermogram of gelatin-g-NVP-AA and gelatin-g-NVP-AA/MMT hydrogels



decomposition gelatin-g-NVP-AA with  $\Delta H$  1.71 J g<sup>-1</sup>. Also, two small peaks were seen in the gelatin-g-NVP-AA/MMT hydrogel thermogram in 355.2 and 491.1 °C which resulted of melting and degradation of gelatin-g-NVP-AA/MMT hydrogel with  $\Delta H$  12.3 and 19.2 J g<sup>-1</sup>, respectively [61]. The DSC thermogram approved MMT in the structure of gelatin-g-NVP-AA/MMT hydrogel dramatically increased the thermal stability of hydrogel.

### Morphology, size and chemical property analysis of hydrogels

By using X-ray powder diffraction (XRD), is possible to phase identification of a crystalline material and prepare information on unit cell dimensions, which determines the ground, homogenized, and average bulk composition. The Fig. 4 shows the XRD pattern of the gelatin, MMT, gelatin-g-NVP-AA and gelatin-g-NVP-AA/MMT nanocomposite hydrogels. As shown in Fig. 4, the pure MMT showed a base peak in  $2\theta = 7.48^\circ$  which referred to the conforming of the interlamellar distance (at the direction of 001) and the basal plane (Ref.00-029-1771). The gelatin had no peak in XRD,

while gelatin-g-NVP-AA had a broad peak in  $2\theta = 24^\circ$  which was related to the amorphous structure of gelatin and hydrogel. The XRD pattern of gelatin-g-PVP-AA/MMT showed a small peak in  $2\theta = 7.48^\circ$  which confirmed the existence the MMT onto chains entrance in empty space of nanocomposite hydrogel, and two peaks in  $2\theta = 24^\circ$  and  $2\theta = 33^\circ$  which are related to the amorphous structure of nanocomposite hydrogel. In addition, other peaks of MMT disappeared in gelatin-g-NVP-AA/MMT XRD pattern which proved the clay layer was dispersed in due to silicate layers' exfoliation [62]. This high dispersion of clay layer into the matrix of hydrogel was the necessary factor to approve the well-exfoliated nanocomposite hydrogel that this effect was shown in TEM image [32].

Also, for more analysis of size and morphology, gelatin-g-PVP-AA/MMT nanocomposite was analyzed by TEM and DLS (Fig. 5). The TEM image showed the spherical MMT with higher density was dispersed in gelatin-g-PVP-AA which detected size for MMT was about 50–110 nm (Fig. 5a). In addition, DLS analysis of gelatin-g-NVP-AA/MMT illustrated particles size were between 40 and 130 nm that average size of the particle was in 85 nm (Fig. 5b). In addition, the BET isotherm test showed the mean average pores diameter

**Fig. 4** XRD patterns of the gelatin, MMT, gelatin-g-NVP-AA and gelatin-g-NVP-AA/MMT

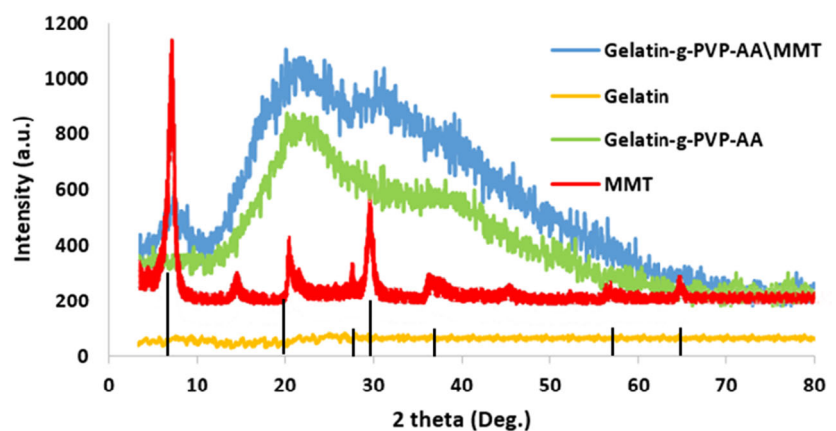
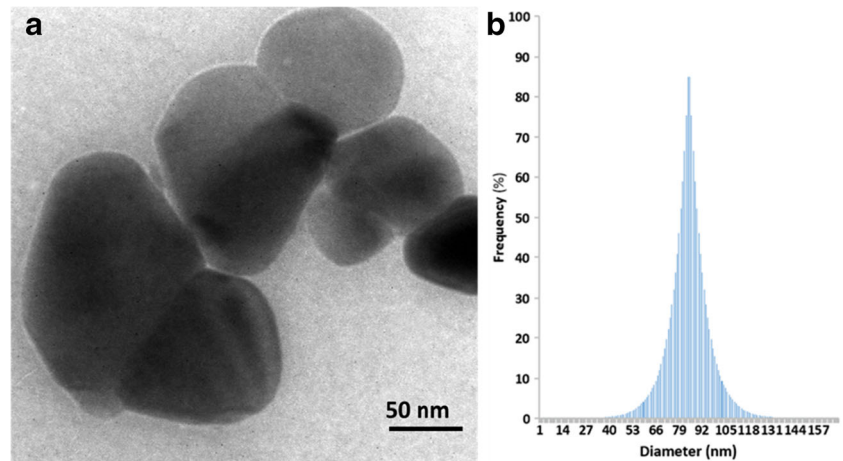


**Fig. 5** TEM image (a) and DLS analysis of (b) gelatin-g-PVP-AA/MMT nanocomposite



was 2.41 nm and the active surface area of gelatin-g-NVP-AA/MMT was expected  $2.4571 \text{ m}^2 \text{ g}^{-1}$ .

For approving the elemental analysis, size and morphology of cross-link gelatin-g-NVP-AA and gelatin-g-NVP-AA/MMT nanocomposite hydrogels were used energy-dispersive X-ray spectroscopy (EDX) and scanning electron microscope (SEM). By using EDX technique could be analyzed the atomic

proportion which was used in a particle. As shown in Fig. 6 could be identified the elements were contained in the structure of gelatin-g-NVP-AA and gelatin-g-NVP-AA/MMT nanocomposite hydrogels, respectively. The Fig. 6a showed gelatin-g-NVP-AA hydrogel contains C, N and O with 42.1, 40.9 and 16.2%, respectively and negligible amount of Na. The Fig. 6b approved the MMT nanocomposites were grafted

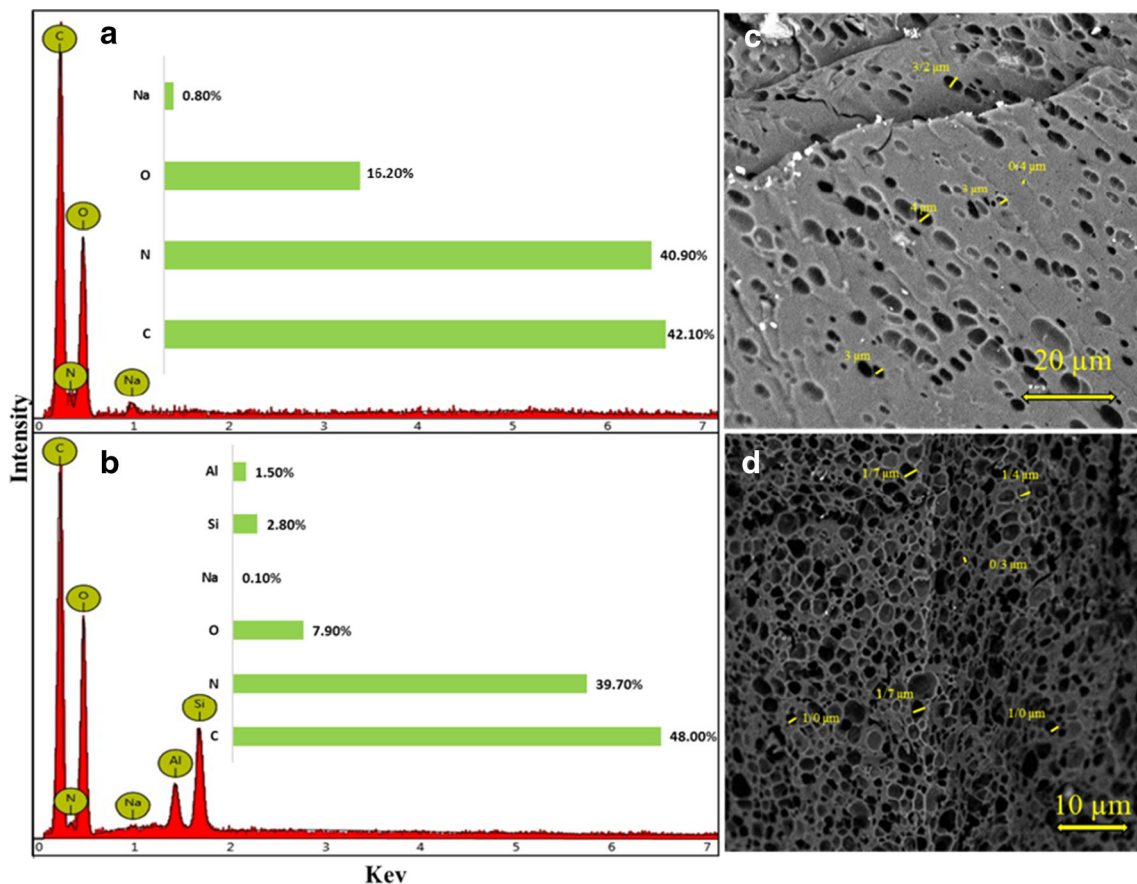


**Fig. 6** EDX analysis of gelatin-g-NVP-AA (a), gelatin-g-NVP-AA/MMT nanocomposite (b), SEM images of gelatin-g-NVP-AA (c), gelatin-g-NVP-AA/MMT nanocomposite (d)



in gelatin-g-NVP-AA/MMT nanocomposite hydrogel by illustrating the 1.5% Al, 2.8% Si, 7.9% N, 39.7% O, and 48% C in the structure.

The Fig. 6c-d illustrated the SEM image of gelatin-g-NVP-AA and gelatin-g-NVP-AA/MMT nanocomposite hydrogels, respectively which showed the size and topology of them. The SEM images of gelatin-g-PVP-AA (Fig. 6c) and gelatin-g-NVP-AA/MMT nanocomposite (Fig. 6d) hydrogels exhibited the surface of components had highly porous surface in gelatin-g-NVP-AA/MMT nanocomposite to gelatin-g-NVP-AA. The average detected size of pores in Fig. 6c and d were about 0.4–4.0  $\mu\text{m}$  and 0.3–1.7  $\mu\text{m}$ , respectively which indicated gelatin-g-NVP-AA/MMT nanocomposite had smaller pore than gelatin-g-NVP-AA could be more effective in swelling and drug loading. In addition, the Fig. 7a-b showed the amount of contain in hydrogels after drug loading.

The Fig. 7a showed gelatin-g-NVP-AA/Ce hydrogel had C, N, O, Na and S with 30.07, 1.64, 44.36, 22.57 and 1.36%, respectively which confirmed the loading of cephalexin on hydrogel by present of S in the contain of the structure. The Fig. 7b approved the MMT nanocomposites and cephalexin were grafted in gelatin-g-NVP-AA/MMT/Ce nanocomposite hydrogel by illustrating the 1.5% Al, 2.8% Si, 7.9% N, 39.7% O, and 23.7% C, 1.2% N, 35.2% O, 37.7% Na, 0.7% Al and

1.37% S in its structure. The Fig. 7c-d showed the morphology and size of particles after loading of drugs which showed cubic morphology for particles with average identified size about 10–50 nm and 30–60 nm for gelatin-g-NVP-AA (Fig. 6c) and gelatin-g-NVP-AA/MMT nanocomposite hydrogels (Fig. 6f), respectively.

## Swelling study

### Salts effect on swelling of hydrogels

Swelling capacity of nanocomposite hydrogels in different salt solutions decreased significantly compared with the amount of swelling in distilled water.

As shown in Fig. 8, in different solution gelatin-g-NVP-AA/MMT nanocomposite in compare to gelatin-g-NVP-AA had increased in swelling. Also, by comparing periodic calculations on a series of monovalent ( $\text{Li}^+$ ,  $\text{Na}^+$ ,  $\text{K}^+$ ,  $\text{Rb}^+$ ,  $\text{Cs}^+$ ), divalent ( $\text{Mg}^{2+}$ ,  $\text{Ca}^{2+}$ ,  $\text{Sr}^{2+}$ ,  $\text{Ba}^{2+}$ ) and trivalent cations ( $\text{Al}^{3+}$ ) and monitoring their effect on the swelling of hydrogels illustrated adsorbing water increased with increasing cation radius in one series and swelling reduced with number of charges in one row cations ( $\text{Na}^+$ ,  $\text{Ca}^{2+}$ ,  $\text{Al}^{3+}$ ).

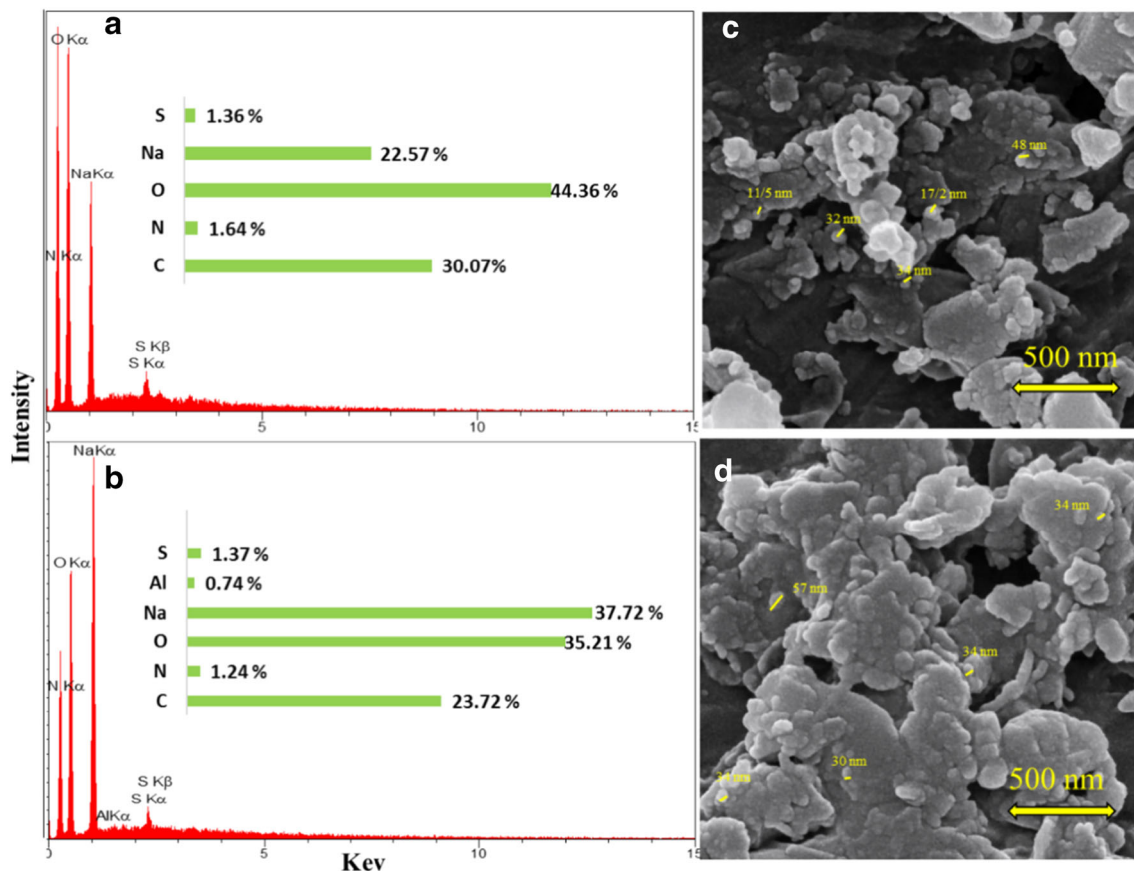
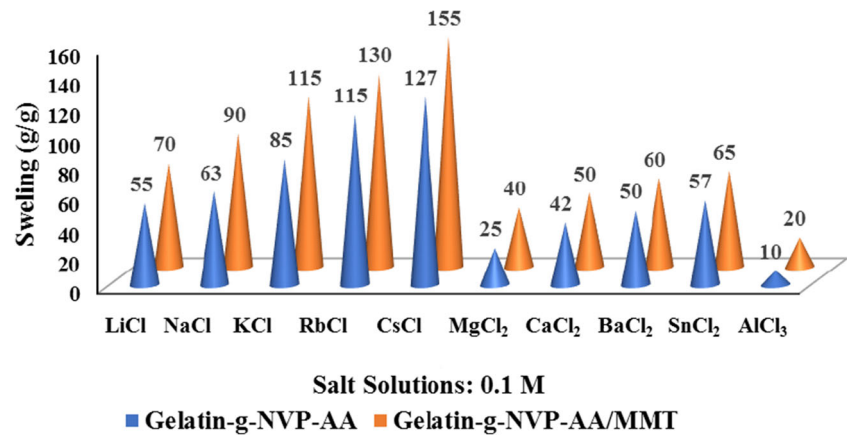


**Fig. 7** EDX analysis of gelatin-g-NVP-AA/Ce (a), gelatin-g-NVP-AA/MMT/Ce nanocomposite (b), SEM images of gelatin-g-NVP-AA/Ce (c), gelatin-g-NVP-AA/MMT/Ce nanocomposite (d)

**Fig. 8** Influence capacity of hydrogels swelling in various chlorine salt solutions



This experience revealed ion change had the effect on swelling and this phenomenon could explain by the hard-soft acid-base (HSAB) principles. According to HSAB,  $\text{Na}^+$  that coordinated with  $\text{COO}^-$  in the structure of the hydrogels was hydrated and replaced with another monovalent cation that is softer than  $\text{Na}^+$  and the order of swelling in different monovalent cation was  $\text{Cs}^+ > \text{Rb}^+ > \text{K}^+ > \text{Na}^+ > \text{Li}^+$  [63]. In contrast, by increasing the charge cation in one row, the swelling reduced in the same concentration salt solution and swelling order was  $\text{Na}^+ > \text{Ca}^{2+} > \text{Al}^{3+}$ . For further investigation, the salt solution with different concentrations was used to determine the water absorption in the hydrogels, which indicates that the swelling decreased in the same trend with increasing salt concentration (Fig. 9). The results showed that swelling at gelatin-g-NVP-AA/MMT nanocomposite in the certain cation was more than to gelatin-g-NVP-AA. In addition, with increasing bar charge, the amount of hydrogel density increased and the water absorption decreased because the cross-linking network in the hydrogels was closer to each other and prevented water absorption [32, 64]. Also, groups had repulsion on the hydrogels and increasing in ion strength caused shield electronic repulsion and reduced swelling [3].

### Kinetic study of swelling

Practically using of the hydrogel is related to high swelling at the shortest time. Several factors effects on hydrogel's

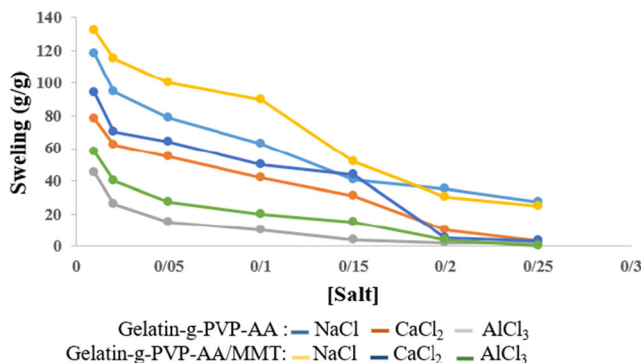


**Fig. 9** The effect of salt concentration on the water absorption hydrogels

swelling as a superabsorbent that Buchholz proposed such as size distribution of powder particles, swelling capacity, specific size area and composition of the polymer [65]. Fig. 10 showed the relation between the swelling and different gelatin-g-NVP-AA and gelatin-g-NVP-AA/MMT nanocomposite hydrogel's particle sizes which indicated absorbing water significantly increased at begging time which emphasized rate of swelling for gelatin-g-NVP-AA/MMT was faster than gelatin-g-NVP-AA, which in continue, swelling obtained at the equilibrium state at about 60 min.

By 'Voigt-based model', could be calculated  $S_t$  (g/g) which is swelling at the time  $t$  by the following equation [66]:

$$S_t = S_e \left( 1 - e^{-t/\tau} \right)$$

Where  $S_e$  is equilibrium swelling (power parameter, g/g), and  $t$  is time (min) for swelling  $S_t$ , and  $\tau$  (min) stand for 'rate parameter'. For particle sizes, 100–250, 250–400 and 400–550  $\mu\text{m}$  in gelatin-g-NVP-AA the rate parameters for superabsorbent was calculated 22.73, 23.53 and 27.93, and in gelatin-g-NVP-AA/MMT was founded 20.45, 21.46 and 26.25,

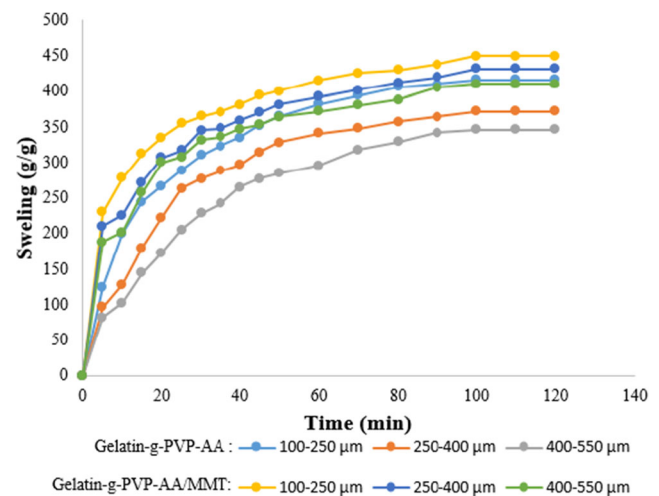


**Fig. 10** Hydrogels swelling kinetics with the different particle size in distilled water

respectively which showed absorbance directly related to particle size. This results exhibited smaller particle size nanocomposite hydrogel swelling more than hydrogel.

### Effect of pH on swelling of hydrogels

Hydrogels in their network have acidic and basic groups, so it is highly sensitive to the pH environment and the amount of water absorption changes in the different pHs. In this investigation, the rate of swelling in gelatin-g-NVP-AA and gelatin-g-NVP-AA/MMT nanocomposite hydrogels at the pH 1 to 13 have been examined (Fig. 11). The amount of ions in water affects the absorption of water, so stock NaOH (13.0) and HCl (1.0) solutions were diluted with distilled water to reach the desired pH. As shown in Fig. 10, swelling gradually increased from pH 1 and reached to maximum point pH 8 which was 177 and 196 (g/g) for gelatin-g-NVP-AA and gelatin-g-NVP-AA/MMT hydrogels respectively, and reduced again at the basic area (pH 9–12). Because the carboxylate groups mostly changed to in the form of nonionic hydrophilic COOH and –OH groups in the acidic media (pH 1–5), the swelling values of hydrogels were not too much, but by increasing pH of solutions from 6 to 8 the rate of hydrogel’s swelling significantly increased as the pH of solutions was increased from 4 to 8 which repulsion between carboxylate groups after ionization made an increase in the swelling value. The reducing swelling ratio in the strong basic solutions (pH 8–13) was affected by excess Na<sup>+</sup> in the solution which prevented anion–anion carboxylate anions repulsion [67].

### Drug loading and releasing study

#### Drug loading study

Hydrogels have high absorbance properties due to their pore size cavities on their surface. For this purpose, synthetic hydrogels were tested for cephalixin absorption to show how much of the drug could be loaded on the hydrogels. To measure the drug loaded, 0.1 g of gelatin-g-NVP-AA and

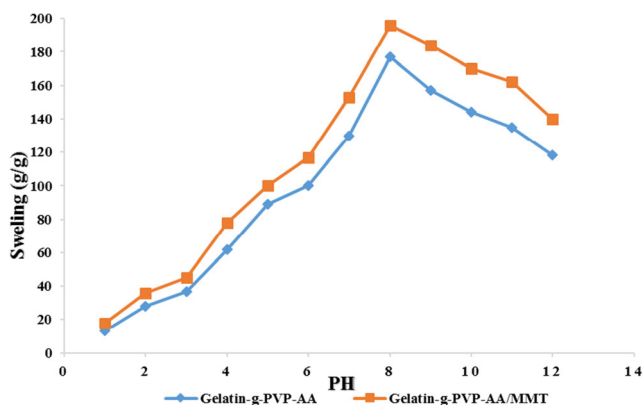


Fig. 11 Effect of pH solutions on the capacity of hydrogels swelling

gelatin-g-NVP-AA/MMT hydrogels nanocomposite were kept in 200 ppm solution of drug for 24 h to absorb drug from in distilled water. Then, the total amount of drug loaded on the hydrogels was measured from on loaded drug in filtrate solution (Fig. 12). The result exhibited gelatin-g-NVP-AA and gelatin-g-NVP-AA/MMT hydrogels nanocomposite significantly absorbed 160 (80%) and 175 (88%) drug from distilled water, respectively which showed hydrogels could be used efficiently for further examination.

### The effect of nanoclay in drug loading in nanocomposite hydrogel

In this part of the study, the amount of nanoclay was evaluated for drug adsorption in nanocomposite hydrogel. As the SEM image showed, the amount of porous surface in gelatin-g-NVP-AA/MMT nanocomposite hydrogel was increased with the addition of nanoclay to the hydrogel which caused to improve the amount of inflammation and the penetration of the water-soluble drug increases into the nanocomposite’s hydrogel network, which increased the concentration of the drug inside the hydrogel network. As the absorption curve showed (Fig. 13), increasing the concentration of MMT to the hydrogel and forming the nanocomposite hydrogel caused the amount of drug loading was increased to 0.008 g / MMT, but after that, the excess amount of MMT reduced the drug loading, which could be due to the filling of empty spaces nanocomposite hydrogel by ineffective amount of MMT. The results of this investigation were given in Table 2. These results indicated that the amount of MMT plays an important role in the amount of drug loading in the nanocomposite hydrogel.

### The effect of drying the hydrogel at different temperatures for loading drug

The drying rate will change the surface and structure and way the particles are stacked together. By changing the structure, the absorption of the drug in the hydrogels will

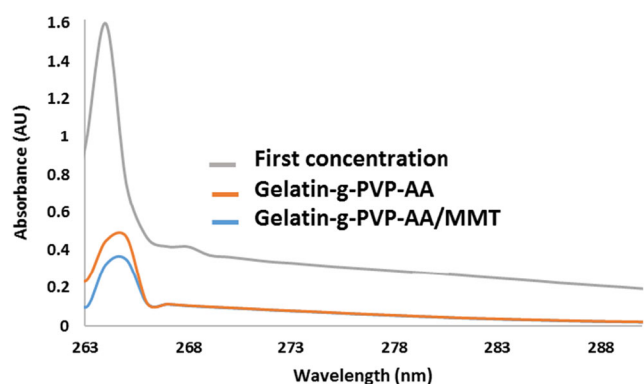
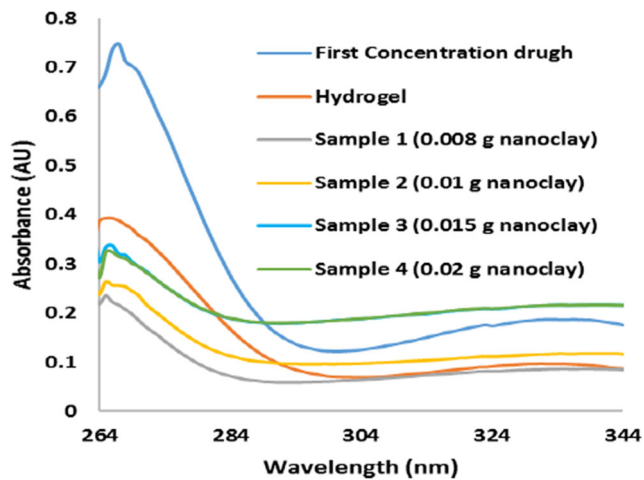


Fig. 12 Absorption spectra of loaded drug on hydrogels in distilled water



**Fig. 13** Absorption spectra of drug loading in nanocomposite hydrogels with different values of nanoclay

be different. For this reason, synthetic hydrogels were dried at different temperatures and the absorption of drug was studied. The gelatin-g-NVP-AA and gelatin-g-NVP-AA/MMT nanocomposite hydrogels were dried at 25, 60, 70 and 80 °C and 0.1 g of them were put in 150 ppm solution of drug for 24 h. After that, the hydrogels were filtered and filtrate was used to calculate the total amount of drug loaded by UV spectroscopy. As shown in Fig. 14, the drug loading on hydrogels was decreased by increasing the temperature. The amount of loaded drug on the gelatin-g-NVP-AA was 61, 50, 41 and 26% (Fig. 14a) and on the gelatin-g-NVP-AA/MMT was 87, 66, 52, 39% (Fig. 14b) at 25, 60, 70 and 80 °C, respectively. The result indicated that increasing the temperature caused to aggregate hydrogels and reduce the pores on the surface which resulted to reduce drug loading on the hydrogels.

### The effect of ion valence number in drug loading

Several studies have shown that the rate of hydrogel swelling is strongly influenced by the properties of solutions, such as the type of soluble salts, the concentration of soluble salts, and ion charge ratios. As shown in Fig. 15, the amount of drug trapped into hydrogels in a saline solution containing NaCl was higher

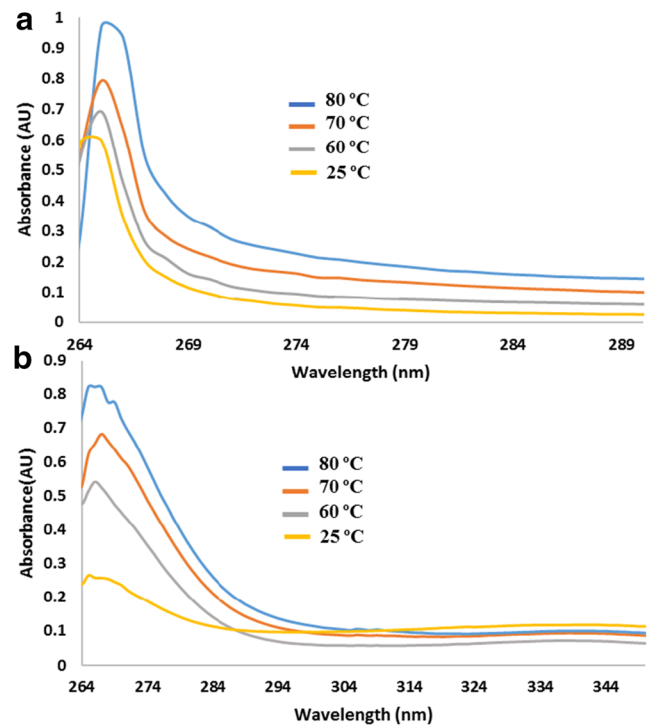


**Fig. 14** Absorption spectra of drug loading in dryness hydrogels in different temperature

than  $\text{CaCl}_2$  and  $\text{AlCl}_3$ , and the amount loaded in the gelatin-g-NVP-AA/MMT nanocomposite hydrogel was greater than the gelatin-g-NVP-AA hydrogel in these salts. In solutions containing NaCl,  $\text{CaCl}_2$  and  $\text{AlCl}_3$ , the amount of loaded drug onto the gelatin-g-NVP-AA hydrogel were 30.1, 22.4 and 12.3% and for the gelatin-g-NVP-AA/MMT nanocomposite hydrogel were 55.2, 39.4 and 18.8%, respectively. The main reason for the drop in inflation hydrogels demonstrated to the overlapping effect of the cations, which caused to reduce the electrostatic anion-anion repulsion. As a result, the difference in osmotic pressure was reduced because of the difference in the concentration the moving ions between the hydrogels and the aqueous phase. In addition, high ionic valence number cations by creating a network of ions at the hydrogels which greatly reduced the absorption of water and the rate of inflation of the hydrogels, and for this two reasons, a lower amount of drug trapped in the porous of the hydrogel [64].

**Table 2** Drug loading rate in different samples of nanocomposite hydrogels with different amounts of nanoclay

Samples	MMT(g)	Es(g/g)	Initial drug concentration (ppm)	Loading(ppm)	% Loading
Hydrogel	–	450	80	33.1	60
1	0.008	557	80	68.2	85
2	0.01	544	80	65.5	82
3	0.015	515	80	56.0	70
4	0.02	515	80	56.0	70



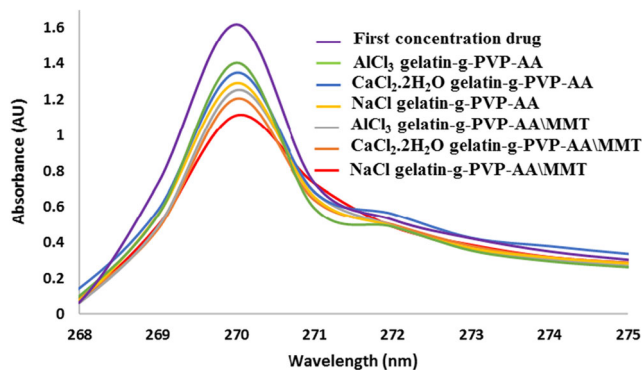


**Fig. 15** Adsorption spectra of the rate of drug loading in different salt solutions

### Evaluation of the drug loading in hydrogels by UV-Vis spectroscopy in universal buffer

In this part of experiment drug loading in the gelatin-g-PVP-AA and gelatin-g-NVP-AA/MMT nanocomposite hydrogels at different pH (1–12) after 6, 12, 24 and 48 h were investigated. As Table 3 shown, the maximum amount of loading drug was 61.5% for gelatin-g-NVP-AA and for gelatin-g-NVP-AA/MMT was 81.3% in pH = 7 after 48 h, respectively. By increasing the time, the drug loading on hydrogels was increased, and also the order of loading in different pHs was 7 > 5 > 8 > 10 > 12 > 3 > 1. The result indicated that in neutral condition the surface of hydrogels was more reactive to absorb drug because of making zwitter ionic structure between cephalixin and hydrogel functional groups.

### Evaluation of the drug releasing from hydrogels in different buffers

In order to select the best buffer solution for subsequent testing, the drug releasing rate was evaluated in three types of buffer salt, universal [58] and stock that the results were shown in Fig. 16. As the results showed, the universal buffer

had the least interaction with different pHs Cephalixin at  $\lambda_{max} = 250\text{--}280\text{ nm}$ , and the universal buffer was used as a reference to continue the experiments.

### Temperature effect on the drug releasing of hydrogels

To observe the temperature effect on the amount of the drug releasing in the loaded gelatin-g-NVP-AA and gelatin-g-NVP-AA/MMT nanocomposite hydrogels, the amount of the individual samples was placed in the buffer solution at three different temperatures over a specified time. As it is evident from the Fig. 17a and b, the highest amount of the drug releasing in both samples occurred at the highest temperature (43 °C). With increasing temperature, the speed of the drug molecules in the hydrogels was increased and the rate of release increased. The results showed that with increasing temperature, the drug releasing in the gelatin-g-NVP-AA/MMT nanocomposite (Fig. 17b) was higher than the gelatin-g-NVP-AA (Fig. 17a), which could be due to increasing the size and reactivity of nanoclay particles and reducing the available space for drug loaded on the nanocomposite hydrogels. According to these results, the amount of drug releasing was 47.5, 51.5 and 55.8% for the gelatin-g-NVP-AA (160 ppm loaded drug) and 50.5, 54.0 and 59.0% for the gelatin-g-NVP-AA/MMT nanocomposite (175 ppm loaded drug) at 25, 35 and 43 °C, respectively.

### Time effect on the drug releasing at different pH

The drug releasing rate varies in different pH due to the different structure of the hydrogels. For this reason, the effect of time was investigated on the amount of drug releasing from gelatin-g-NVP-AA and gelatin-g-NVP-AA/MMT nanocomposite hydrogels in constant and different pHs.

The releasing drug from gelatin-g-NVP-AA and gelatin-g-NVP-AA/MMT nanocomposite hydrogels was increased over time from 6 to 48 h (Fig. 18). The amount of released drug

**Table 3** Loading drug for gelatin-g-NVP-AA and gelatin-g-NVP-AA/MMT at different pH in distilled water

pH	gelatin-g-NVP-AA				gelatin-g-NVP-AA/MMT											
	Con. Loading (ppm)				Loading (%)				Con. Loading (ppm)				Loading (%)			
	6 h	12 h	24 h	48 h	6 h	12 h	24 h	48 h	6 h	12 h	24 h	48 h	6 h	12 h	24 h	48 h
1	0	0	1.2	1.2	0	0	2.4	2.4	1.6	2.1	3.1	3.1	3.2	4.3	6.2	6.2
3	8.1	9.6	11.5	11.5	16.2	19.2	23.0	23.0	13.2	14.2	15.3	16.0	26.5	28.5	30.6	32.0
5	10.1	18.3	25.2	28.4	20.2	36.0	50.4	56.2	22.4	30.3	32.1	34.2	44.2	60.3	64.0	68.5
7	19.3	24.5	29.1	30.7	38.6	49.0	58.2	61.5	25.0	32.0	37.1	40.6	50.0	64.0	74.3	81.3
8	12.1	20.5	24.7	26.1	24.2	41.1	49.5	52.3	22.6	27.6	29.7	31.6	45.3	55.2	59.4	63.3
10	11.1	14.5	17.5	21.1	22.3	29.1	35.0	42.2	19.0	23.6	25.6	27.0	38.0	47.3	51.2	54.0
12	8.7	11.3	15.0	15.0	17.5	22.6	26.0	30.0	13.0	17.2	19.0	20.7	26.0	34.5	38.0	41.5

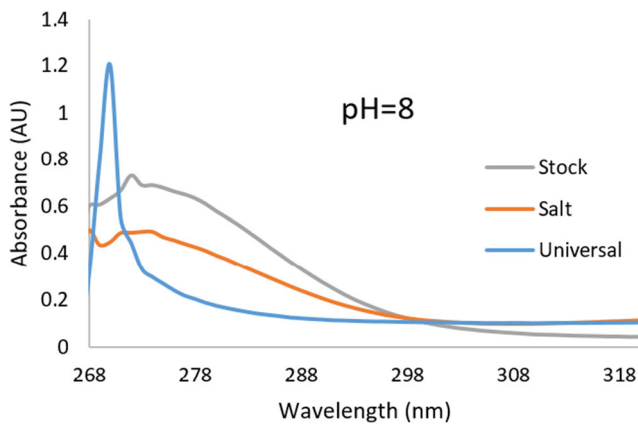


**Fig. 16** Absorption spectra of the drug releasing in different buffers (pH = 8)

was 47, 54, 61 and 76% for gelatin-g-NVP-AA (Fig. 18a) and 58, 64, 78 and 88% for gelatin-g-NVP-AA/MMT (Fig. 18b) in 6, 12, 24 and 48 h, respectively. Therefore, with the passage of time the releasing drug became more and more and in case of gelatin-g-NVP-AA/MMT was greater than gelatin-g-NVP-AA nanocomposite hydrogels.

Cephalexin and hydrogels having the carboxylic acid group in their structure and in alkaline medium changed to carboxylate groups which caused the electrostatic repulsion between the two compounds because of the same charges and increased the rate of the drug release. Also, the results showed that by increasing the amount of water absorption in the hydrogels, the drug was increased in proportion to its release, and changing the pH was in

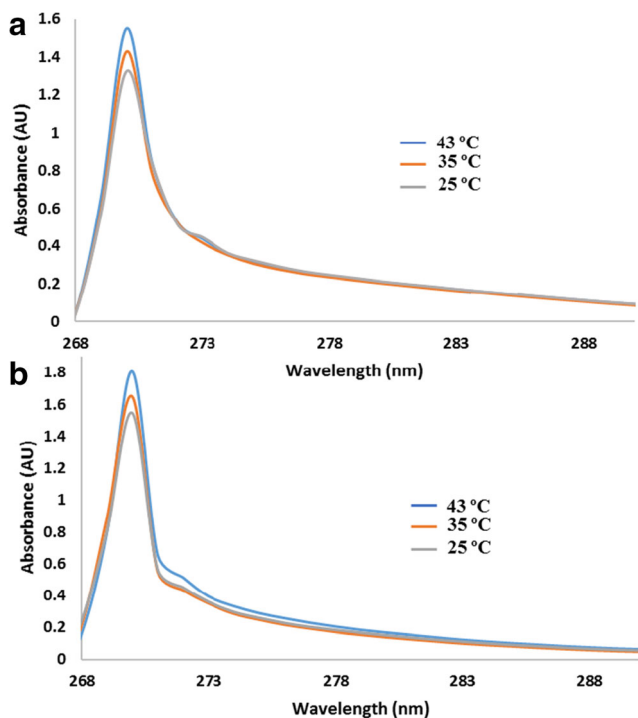


**Fig. 17** Temperature effect on absorption spectra of the drug releasing (a) gelatin-g-NVP-AA, (b) gelatin-g-NVP-AA/MMT

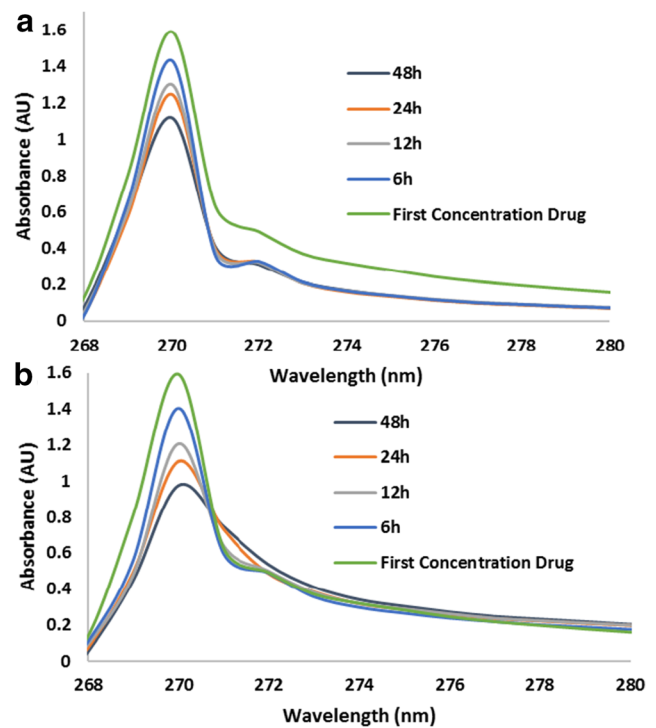


**Fig. 18** Time effect on absorption spectra of the drug releasing (a) gelatin-g-NVP-AA, (b) gelatin-g-NVP-AA/MMT

the same direction in both the effect and that was  $\text{pH } 8.0 > 10 > 7$ . As could be seen in Fig. 18, the amount of cephalexin release was much higher in basic solution in comparison with acidic media that result could be the effect on changing the interaction between cephalexin and polymer network [60].

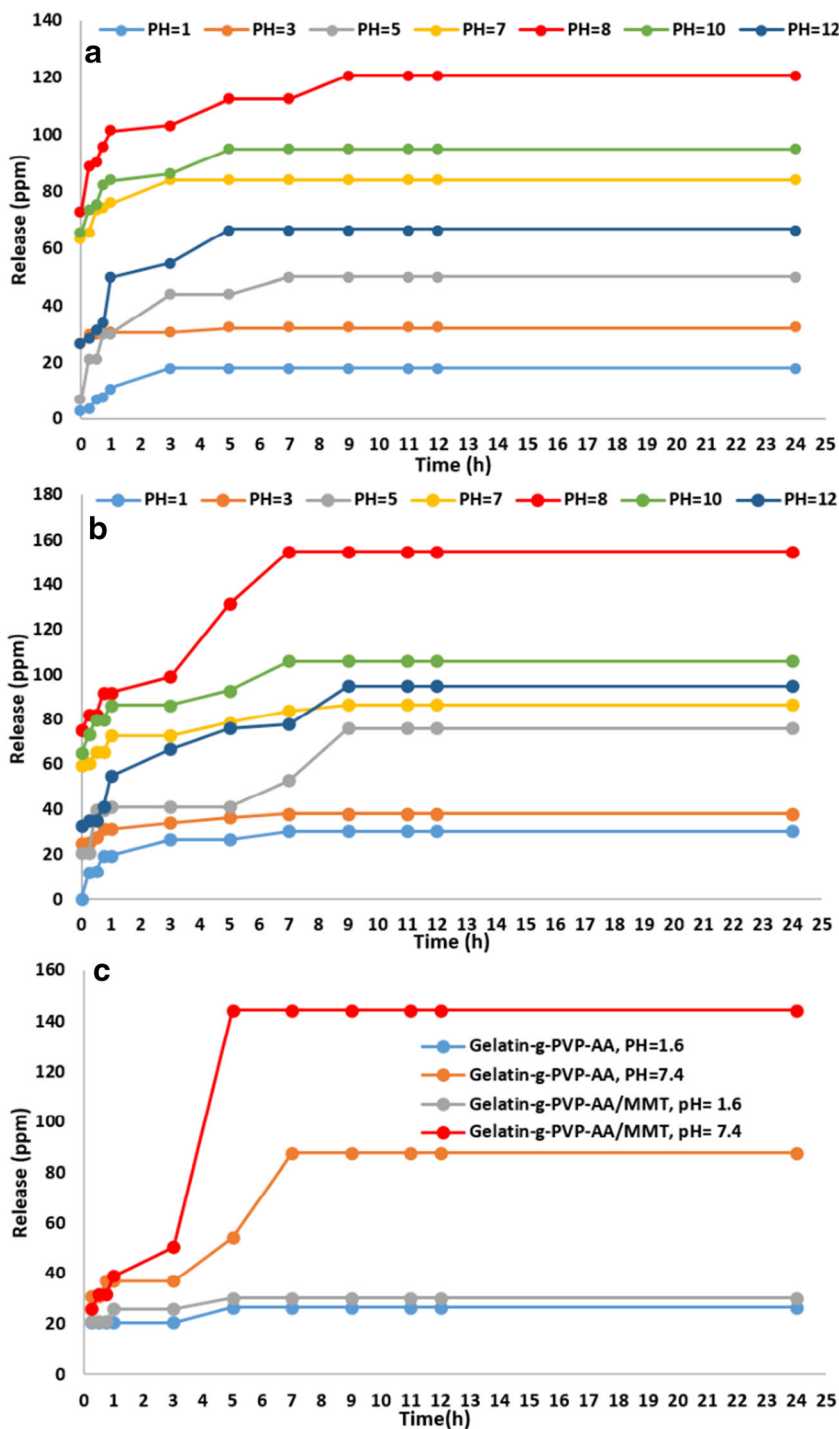
It was notable that the results obtained the concentration of the drug releasing for all of pH was constant after 9 h, and the maximum amount of the drug releasing was 120 ppm and 140 at pH 8 for the gelatin-g-NVP-AA and gelatin-g-NVP-AA/MMT nanocomposite hydrogels respectively, and after that until 24 h the concentration of the released drug was the same (Fig. 19a, b).

In addition, the amount of the drug releasing in the similar body condition was examined in over time that the results showed the release rate in pH 7.4 (intestinal condition) was far higher than pH 1.6 (stomach condition) for the gelatin-g-NVP-AA and gelatin-g-NVP-AA/MMT nanocomposite hydrogels (Fig. 19c). These results suggested that this protective system was an ideal method for transferring the cephalexin into the intestine and increase the efficiency of the medicine, which is susceptible to acidic conditions in the stomach.

### Evaluation of the drug releasing from hydrogels by UV-Vis spectroscopy

The UV-Vis spectroscopy is a convenient method for measuring compounds that are absorbed in this region, and cephalexin is sensitive in this method due to the presence

**Fig. 19** The drug releasing curve relative to time in different pH for gelatin-g-NVP-AA (a), gelatin-g-NVP-AA/MMT (b) and in vitro test (c)



of a phenyl group in its structure, and the amount of releasing-drug is measurable. Initially, the universal buffer solution in different pH was mixed with different concentrations drug solutions and the intensity of absorption was measured by UV spectroscopy. By converting the adsorption intensity to the concentration according to the Beer-Lambert equation, standard curves and line equation for the desired pH were calculated [57].

The results of this study showed that the release of drug from the hydrogels network was directly related to the rate of their inflation in water. The degree of the drug releasing in acidic and high alkaline pHs was very low compared to pH 8. Reducing the drug releasing at acidic pH and the low hydrogels swelling in compare to pH 8 could be due to overlapping of the charge and hydrogen bonding among carboxylic groups in hydrogels and cephalaxin. While in the basic

**Table 4** Determination of the rate of released drug from gelatin-g-NVP-AA and gelatin-g-NVP-AA/MMT at different pH by UV-Vis spectroscopy

pH	gelatin-g-NVP-AA		gelatin-g-NVP-AA/MMT	
	Con. Release (ppm)	Release (%)	Con. Release (ppm)	Release (%)
1	18.1	11.37	30.5	17.3
3	31.9	19.9	37.9	21.5
5	50.0	31.3	76.0	43.3
7	75.8	47.3	86.7	50.0
8	120.9	75.7	154.7	88.1
10	94.9	59.3	106.7	60.7
12	66.8	41.8	96.8	55.1
1.6	27.4	17.0	31.0	18.0
7.4	87.7	54.9	144.4	82.3

medium pH 8, repulsion between carboxylate groups significantly increases hydrogel swelling, as a result, the drug releasing rate reached its maximum. However, in very high pHs, cations that were present in the environment by covering carboxylate groups and forming the ion pair had led to a drop in inflation and the drug release [57]. Also, the release rate of cephalexin in the gelatin-g-NVP-AA/MMT nanocomposite was greater than gelatin-g-NVP-AA hydrogel, which causes more swelling in the water could be due to the sodium ions repulsion in nanoclay. The percentage of released drug was calculated from the following Eq. (2). In this equation,  $L$  and  $R_t$  represent the initial rate of loaded drug (210 ppm) and the amount of released drug at time  $t$ .

$$\%Drug\ release = \frac{R_t}{L} \quad (2)$$

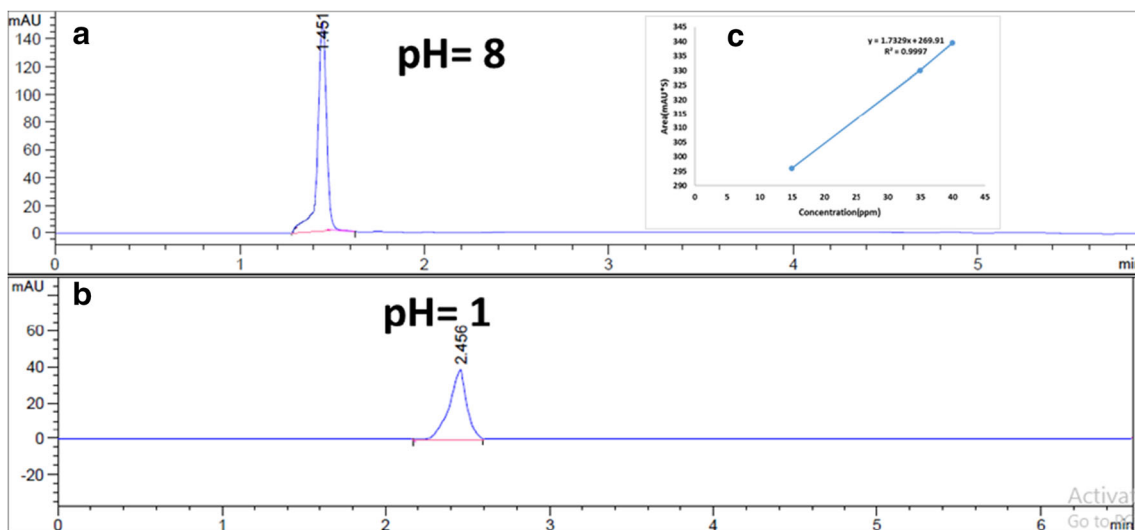
The results showed that the highest drug releasing was related to pH 8 that the drug releasing rate at pH 8 was 129.9 and 154.7 ppm, and the percentage of release was

calculated to be 75.7 and 88.1% for gelatin-g-NVP-AA and gelatin-g-NVP-AA/MMT, respectively (Table 4).

Also, the release of cephalexin was performed according to the method described in universal buffer with pH 7.4 and pH 1.6 at constant temperature (37 °C), similar to the stomach and intestinal conditions. As the results showed, the amount of released drug at pH 7.4 was higher than pH 1.6, as well as gelatin-g-NVP-AA/MMT nanocomposite more than gelatin-g-NVP-AA and hydrogels due to higher inflation.

### Evaluation of the drug loading and releasing of hydrogels by HPLC

In order to verify the drug loaded onto the gelatin-g-PVP-AA and gelatin-g-NVP-AA/MMT nanocomposite hydrogels and the drug releasing them, chromatography HPLC C18 column was used with a length of 10 cm and run for 10 min with acetonitrile\universal buffer (83:17) as an eluent at  $\lambda_{max} = 250\text{--}280$  nm in order to determine cephalexin in a HPLC

**Fig. 20** Chromatogram HPLC cephalexin loaded on gelatin-g-NVP-AA (a), gelatin-g-NVP-AA/MMT (b) and the calibration curve (c) in pH 8



**Table 5** The rate of released drug from gelatin-g-NVP-AA (A), gelatin-g-NVP-AA/MMT at different pH

pH	gelatin-g-NVP-AA		gelatin-g-NVP-AA/MMT	
	Con. Release (ppm)	Release (%)	Con. Release (ppm)	Release (%)
1	16.7	10.9	20.6	12.2
3	29.5	19.3	34.0	20.0
5	56.1	38.8	70.3	41.5
7	73.6	48.3	84.7	50.0
8	102.7	67.4	146.0	86.2
10	85.5	56.1	111.4	65.8
12	60.5	39.7	98.0	57.8
1.6	19.8	12.9	24.6	14.6
7.4	84.1	55.2	128.3	75.7

column that this method was more accurate than measuring with UV/Vis spectroscopy. Initially, the gelatin-g-NVP-AA and gelatin-g-NVP-AA/MMT nanocomposite hydrogels were kept at drug solution (200 ppm) for 24 h and after filtration, the filtrate was used to detect amount of loading drug. The result showed the loading drug on the gelatin-g-NVP-AA and gelatin-g-NVP-AA/MMT nanocomposite hydrogels were 159.6 ppm (79.8%) and 175.5 ppm (87.7%), respectively.

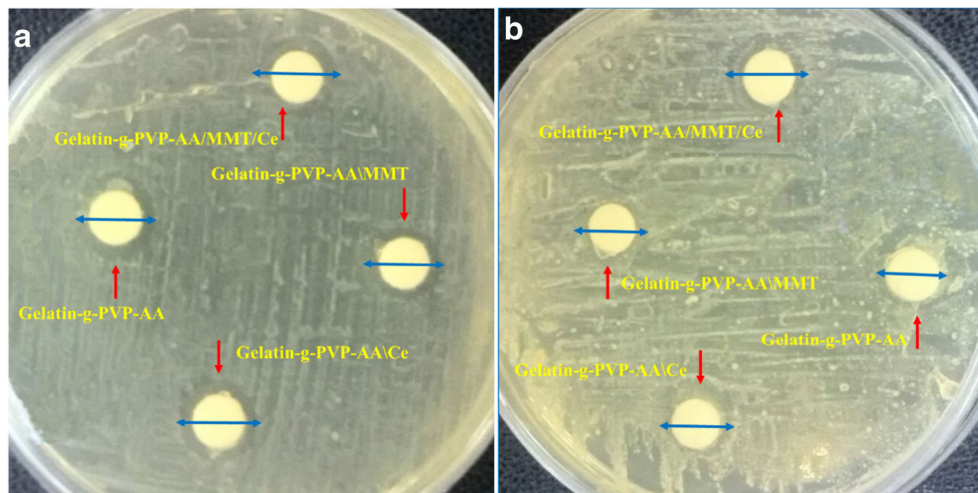
In continues of this research, to prepare the standard curve, different drug concentrations in various pH were prepared and injected into the HPLC column. The calibration curve was plotted based on the concentration of drug to the subsurface in a chromatogram (HPLC) and by using the linear equation obtained through the calibration curve; it was easy to calculate the drug concentration (Fig. 19c).

Firstly, the HPLC spectrum of pure cephalexin showed a peak 3.136 min which expected other peaks reveal before this time. In continues, the drug releasing from the hydrogels were evaluated at different pH after a specific time that Fig. 19 (S 19–27) showed the cephalexin

absorption was at the peak time of 1.451 and 2.456 min in pH 1 after releasing from gelatin-g-NVP-AA (Fig. 19a) and gelatin-g-NVP-AA/MMT nanocomposite hydrogels (Fig. 19b), respectively.

As shown in Fig. 20, the amount of released drug from gelatin-g-NVP-AA/MMT (146.0, 86.2%) was greater than gelatin-g-NVP-AA (102.7, 67.4%), which could be attributed to the presence of MMT in a nanocomposite hydrogel network which, by increasing its activity in the hydrogel network caused to release further than hydrogel. In addition, it was noteworthy that the highest drug releasing occurred at pH 8. Also, the drug releasing in similar conditions of the human body was carried out in a solution with pH 1.6 (stomach condition) and pH 7.4 (intestinal condition) of the gelatin-g-NVP-AA and gelatin-g-NVP-AA/MMT nanocomposite hydrogels and their release rate were measured and result showed releasing in pH 7.4 (intestinal condition) was greater than pH 1.6 (stomach condition) in both samples of the hydrogels. The results of the drug releasing study by the HPLC method were shown in Table 5.

**Fig. 21** Antibacterial activities of the gelatin-g-NVP-AA, gelatin-g-NVP-AA/MMT, gelatin-g-NVP-AA/Ce and gelatin-g-NVP-AA/MMT/Ce hydrogels against *S. aureus* (a) and *E. coli* (b)



## Antibacterial activities

The synthesized hydrogels were investigated for in vitro antibacterial effect against the gram-positive *Staphylococcus aureus* and the gram-negative *Escherichia coli* by comparing the diameter inhibition zones of the growth. The Fig. 20 illustrated that gelatin-g-NVP-AA, gelatin-g-NVP-AA\MMT and gelatin-g-NVP-AA\MMT\Ce hydrogels had antibacterial effect on *S. aureus* and *E. coli* bacteria and after 24 [68]. After measured the inhibition zone the paper discs soaked exhibited 33.4 mm, 33.6 mm, 35.0 mm and 37.0 mm (Fig. 21a) for the gelatin-g-NVP-AA, gelatin-g-NVP-AA\MMT, gelatin-g-NVP-AA\Ce and gelatin-g-NVP-AA\MMT\Ce hydrogels against *S. aureus* and 29.2 mm, 30.6 mm, 30.6 mm and 34.6 mm against *E. coli* (Fig. 21b), respectively. As result showed, all samples illustrated antibacterial activity against both bacteria because of bioactivity of the hydrogels structure but the loaded drug nanocomposite hydrogel (gelatin-g-NVP-AA\MMT\Ce) showed further potential antibacterial activity than the other hydrogels under same test conditions. This effect could be due to the swelling from the agar and the drug releasing from the porous surface nanocomposite hydrogel and more interaction with cell wall bacteria.

## Conclusion

In this investigation, the free radical method was used to synthesis of gelatin base of cross-linking poly vinyl/acrylic acid hydrogel and nanoclay hydrogel which had huge inflation with 450 and 557 (g/g) for gelatin-g-NVP-AA and gelatin-g-NVP-AA/MMT nanocomposite hydrogels, respectively. These hydrogels were used to load cephalexin as an antibacterial drug and characterized by IR spectroscopy to confirm its structure onto hydrogels. The TGA and DSC analyses showed these hydrogels had a good thermal stability (550 °C) and gelatin-g-NVP-AA/MMT nanocomposite hydrogel due to had MMT in its structure, this effect was greater than and gelatin-g-NVP-AA/MMT nanocomposite hydrogel. Also, the XRD pattern and TEM image approved that MMT layers in hydrogel nanocomposite were separated and exfoliated. The DLS analysis showed the average size of nanocomposite hydrogels was 85 nm. In addition, the SEM images illustrated that in hydrogels structure had porous morphology on their surface before the drug loading and nano particle size and their morphology after drug loading that these pores directly affected on swelling, drug loading and drug releasing. The amount of adsorption of the synthesized hydrogels in salt solutions was strongly reduced in contrast to water. Also, in the kinetic study of inflation showed the rate of swelling hydrogels increased with decreasing particle size. By adding nanoclay to synthesized hydrogel, the absorption capacity of nanocomposite hydrogel dramatically increased and inflationary

behavior depended to the pH and the maximum absorption was at pH 8. Drug loading was investigated in different valence ions and temperature that by increasing ion valence and temperature the drug loading was decreased. Also, the maximum loaded drug on hydrogel was in pH 8 and the 0.008 g of nanoclay in nanocomposite hydrogel. The drug releasing study was done in different buffers, distilled water and pHs which indicated universal buffer in pH 8 had the least interaction with cephalexin and the highest drug releasing that was calculated by UV-Vis spectroscopy and HPLC chromatography. The synthesized gelatin-g-NVP-AA and gelatin-g-NVP-AA/MMT nanocomposite hydrogels and their loaded drug (gelatin-g-NVP-AA\Ce and gelatin-g-NVP-AA/MMT\Ce) were tested against gram-positive *S. aureus* and gram-negative *E. coli* and results showed the gelatin-g-NVP-AA/MMT\Ce nanocomposite hydrogel obtained greater antibacterial activity than the other hydrogels. In totally, we proposed a suitable nanocomposite hydrogel as drug deliver for using against antibacterial diseases.

**Acknowledgements** The authors extend their appreciation to the Azad University of Arak-Iran for financial support of this work.

## References

1. Sultana F, Imran-Ul-Haque M, Arafat M, Sharmin S (2013) An overview of Nanogel drug delivery system. J appl pharm sci 3(9): 95–103. <https://doi.org/10.7324/JAPS.2013.38.S15>
2. Jin S, Liu M, Zhang F, Chen S, Niu A (2006) Synthesis and characterization of pH-sensitivity semi-IPN hydrogel based on hydrogen bond between poly (N-vinylpyrrolidone) and poly (acrylic acid). Polymer 47(5):1526–1532
3. Sadeghi M, Hosseinzadeh H (2008) Synthesis of starch—poly (sodium acrylate-co-acrylamide) superabsorbent hydrogel with salt and pH-responsiveness properties as a drug delivery system. J Bioact Compat Polym 23(4):381–404
4. Kuo C-Y, Don T-M, Lin Y-T, Hsu S-C, Chiu W-Y (2019) Synthesis of pH-sensitive sulfonamide-based hydrogels with controllable crosslinking density by post thermo-curing. J Polym Res 26(1):18
5. Gonçalves C, Pereira P, Gama M (2010) Self-assembled hydrogel nanoparticles for drug delivery applications. Materials 3(2):1420–1460
6. Bhuiyan M, Rahman M, Rahaman M, Shajahan M, Dafader N (2015) Improvement of swelling behaviour of poly (vinyl Pyrrolidone) and acrylic acid blend hydrogel prepared by the application of gamma radiation. Organic Chem Curr Res 4(138):2161–0401.10001
7. Dafader N, Adnan M, Haque M, Huq D, Akhtar F (2011) Study on the properties of copolymer hydrogel obtained from acrylamide/2-hydroxyethyl methacrylate by the application of gamma radiation. Afr J P Appl Chem 5(5):111–118
8. Rizwan M, Yahya R, Hassan A, Yar M, Azzahari AD, Selvanathan V, Sonsudin F, Abouloula CN (2017) pH sensitive hydrogels in drug delivery: brief history, properties, swelling, and release mechanism, material selection and applications. Polymers 9(4):137
9. Sohail K, Khan IU, Shahzad Y, Hussain T, Ranjha NM (2014) pH-sensitive polyvinylpyrrolidone-acrylic acid hydrogels: impact of material parameters on swelling and drug release. Braz J Pharm Sci 50(1):173–184

10. Peppas NA, Hilt JZ, Khademhosseini A, Langer R (2006) Hydrogels in biology and medicine: from molecular principles to bionanotechnology. *Adv Mater* 18(11):1345–1360
11. Jin S, Gu J, Shi Y, Shao K, Yu X, Yue G (2013) Preparation and electrical sensitive behavior of poly (N-vinylpyrrolidone-co-acrylic acid) hydrogel with flexible chain nature. *Eur Polym J* 49(7):1871–1880
12. Richter A, Kuckling D, Howitz S, Gehring T, Arndt K-F (2003) Electronically controllable microvalves based on smart hydrogels: magnitudes and potential applications. *J Microelectromech Syst* 12(5):748–753
13. Bashir R, Hilt J, Elibol O, Gupta A, Peppas N (2002) Micromechanical cantilever as an ultrasensitive pH microsensor. *Appl Phys Lett* 81(16):3091–3093
14. Richter A, Paschew G, Klatt S, Lienig J, Arndt K-F, Adler H-JP (2008) Review on hydrogel-based pH sensors and microsensors. *Sensors* 8(1):561–581
15. Schuvalilo O, Soldatkin O, Lefebvre A, Cespuaglio R, Soldatkin A (2006) Highly selective biosensors for in vivo measurement of glucose, lactate and glutamate. *Anal Chim Acta* 573:110–116
16. Lu Q, Yu J, Gao J, Yang W, Li Y (2011) Glow-discharge electrolysis plasma induced synthesis of Polyvinylpyrrolidone/acrylic acid hydrogel and its adsorption properties for heavy-metal ions. *Plasma Process Polym* 8(9):803–814
17. Yuan Q, Su C, Cao Y, Wu K, Xu J, Yang S (2014) Rhodamine loading and releasing behavior of hydrogen-bonded poly (vinylpyrrolidone)/poly (acrylic acid) film. *Colloids Surf A Physicochem Eng Asp* 456:153–159
18. Sadeghi M (2012) Synthesis of a biocopolymer carrageenan-g-poly (AAm-co-IA)/montmorillonite superabsorbent hydrogel composite. *Braz J Chem Eng* 29(2):295–305
19. Entezami AA, Massoumi B (2006) Artificial muscles, biosensors and drug delivery systems based on conducting polymers: a review. *Iranian Polym J* 15(1):13–30
20. Eroglu B, Dalgakiran D, Inan T, Kurkcuoglu O, Güner FS (2018) A computational and experimental approach to develop minocycline-imprinted hydrogels and determination of their drug delivery performances. *J Polym Res* 25(12):258
21. Razzak MT, Darwis D (2001) Irradiation of polyvinyl alcohol and polyvinyl pyrrolidone blended hydrogel for wound dressing. *Radiat Phys Chem* 62(1):107–113
22. Risbud MV, Hardikar AA, Bhat SV, Bhonde RR (2000) pH-sensitive freeze-dried chitosan–polyvinyl pyrrolidone hydrogels as controlled release system for antibiotic delivery. *J Control Release* 68(1):23–30
23. Marsano E, Bianchi E, Vicini S, Compagnino L, Sionkowska A, Skopińska J, Wiśniewski M (2005) Stimuli responsive gels based on interpenetrating network of chitosan and poly (vinylpyrrolidone). *Polymer* 46(5):1595–1600
24. Pawar RP, Tekale SU, Shisodia SU, Totre JT, Domb AJ (2014) Biomedical applications of poly (lactic acid). *Recent Pat Regen Med* 4(1):40–51
25. Lubasova D, Niu H, Zhao X, Lin T (2015) Hydrogel properties of electrospun polyvinylpyrrolidone and polyvinylpyrrolidone/poly (acrylic acid) blend nanofibers. *RSC Adv* 5(67):54481–54487
26. Kadłubowski S, Henke A, Ulański P, Rosiak JM (2010) Hydrogels of polyvinylpyrrolidone (PVP) and poly (acrylic acid)(PAA) synthesized by radiation-induced crosslinking of homopolymers. *Radiat Phys Chem* 79(3):261–266
27. Kadłubowski S, Henke A, Ulański P, Rosiak JM, Bromberg L, Hatton TA (2007) Hydrogels of polyvinylpyrrolidone (PVP) and poly (acrylic acid)(PAA) synthesized by photoinduced crosslinking of homopolymers. *Polymer* 48(17):4974–4981
28. Ishiduki K, Esumi K (1997) The effect of pH on adsorption of poly (acrylic acid) and poly (vinylpyrrolidone) on alumina from their binary mixtures. *Langmuir* 13(6):1587–1591
29. Jovašević J, Dimitrijević S, Filipović J, Tomić S, Micić M, Suljovrujić E (2011) Swelling, mechanical and antimicrobial studies of Ag/P (HEMA/IA)/PVP semi-IPN hybrid hydrogels. *Acta Phys Polon* 120(2)
30. Bajpai S, Dubey S (2005) In vitro dissolution studies for release of vitamin B12 from poly (N-vinyl-2-pyrrolidone-co-acrylic acid) hydrogels. *React Funct Polym* 62(1):93–104
31. Gallardo A, Eguiburu JL, Berridi MJF, San Román J (1998) Preparation and in vitro release studies of ibuprofen-loaded films and microspheres made from graft copolymers of poly (L-lactic acid) on acrylic backbones. *J Control Release* 55(2–3):171–179
32. Olad A, Zebhi H, Salari D, Mirmohseni A, Reyhanitabar A (2017) A promising porous polymer-nanoclay hydrogel nanocomposite as water reservoir material: synthesis and kinetic study. *J Porous Mater*:1–11
33. Marandi GB, Mahdavinia GR, Ghafary S (2011) Collagen-g-poly (sodium acrylate-co-acrylamide)/sodium montmorillonite superabsorbent nanocomposites: synthesis and swelling behavior. *J Polym Res* 18(6):1487–1499
34. Schexnailder P, Schmidt G (2009) Nanocomposite polymer hydrogels. *Colloid Polym Sci* 287(1):1–11
35. Azmi S, Razak SIA, Abdul Kadir MR, Iqbal N, Hassan R, Nayan NHM, Abdul Wahab AH, Shaharuddin S (2017) Reinforcement of poly (vinyl alcohol) hydrogel with halloysite nanotubes as potential biomedical materials. *Soft Mater* 15(1):45–54
36. Noori S, Kokabi M, Hassan Z (2015) Nanoclay enhanced the mechanical properties of poly (vinyl alcohol)/chitosan/montmorillonite nanocomposite hydrogel as wound dressing. *Procedia Mater Sci* 11:152–156
37. Song L, Zhu M, Chen Y, Haraguchi K (2008) Temperature-and pH-sensitive Nanocomposite gels with semi-interpenetrating organic/inorganic networks. *Macromol Chem Phys* 209(15):1564–1575
38. Abdurrahmanoglu S, Can V, Okay O (2008) Equilibrium swelling behavior and elastic properties of polymer–clay nanocomposite hydrogels. *J Appl Polym Sci* 109(6):3714–3724
39. Huang X, Xu S, Zhong M, Wang J, Feng S, Shi R (2009) Modification of Na-bentonite by polycations for fabrication of amphoteric semi-IPN nanocomposite hydrogels. *Appl Clay Sci* 42(3–4):455–459
40. Zhang Y-T, Zhi T-T, Zhang L, Huang H, Chen H-L (2009) Immobilization of carbonic anhydrase by embedding and covalent coupling into nanocomposite hydrogel containing hydroxalcalcite. *Polymer* 50(24):5693–5700
41. Sirousazar M, Kokabi M, Hassan Z, Bahramian A (2011) Dehydration kinetics of polyvinyl alcohol nanocomposite hydrogels containing Na-montmorillonite nanoclay. *Sci Iran* 18(3):780–784
42. Kaşgöz H, Durmus A (2008) Dye removal by a novel hydrogel-clay nanocomposite with enhanced swelling properties. *Polym Adv Technol* 19(7):838–845
43. Mahdavinia GR, Hasanpour J, Rahmani Z, Karami S, Etemadi H (2013) Nanocomposite hydrogel from grafting of acrylamide onto HPMC using sodium montmorillonite nanoclay and removal of crystal violet dye. *Cellulose* 20(5):2591–2604
44. Kokabi M, Sirousazar M, Hassan ZM (2007) PVA–clay nanocomposite hydrogels for wound dressing. *Eur Polym J* 43(3):773–781
45. Sirousazar M, Kokabi M, Hassan ZM (2011) In vivo and cytotoxic assays of a poly (vinyl alcohol)/clay nanocomposite hydrogel wound dressing. *J Biomater Sci Polym Ed* 22(8):1023–1033
46. Song F, Zhang L-M, Shi J-F, Li N-N (2010) Viscoelastic and fractal characteristics of a supramolecular hydrogel hybridized with clay nanoparticles. *Colloids Surf B* 81(2):486–491
47. Pourjavadi A, Ghasemzadeh H, Soleyman R (2007) Synthesis, characterization, and swelling behavior of alginate-g-poly (sodium acrylate)/kaolin superabsorbent hydrogel composites. *J Appl Polym Sci* 105(5):2631–2639

48. Mahdavinia GR, Aghaie H, Sheykhloie H, Vardini MT, Etemadi H (2013) Synthesis of CarAlg/MMt nanocomposite hydrogels and adsorption of cationic crystal violet. *Carbohydr Polym* 98(1):358–365
49. Siemianowski LA, Rosenheck JP, Whitman CB (2014) Nalbuphine-induced psychosis treated with naloxone. *Am J Health Syst Pharm* 71(9):717–721. <https://doi.org/10.2146/ajhp130485>
50. Chouhan R, Bajpai AK (2010) Release dynamics of ciprofloxacin from swellable nanocarriers of poly(2-hydroxyethyl methacrylate): an in vitro study. *Nanomed Nanotech Bio Med* 6(3):453–462. <https://doi.org/10.1016/j.nano.2009.11.006>
51. Mostafavi A, Emami J, Varshosaz J, Davies NM, Reza zadeh M (2011) Development of a prolonged-release gastroretentive tablet formulation of ciprofloxacin hydrochloride: pharmacokinetic characterization in healthy human volunteers. *Int J Pharm* 409(1):128–136. <https://doi.org/10.1016/j.ijpharm.2011.02.035>
52. Singh B, Sharma V (2017) Crosslinking of poly(vinylpyrrolidone)/acrylic acid with tragacanth gum for hydrogels formation for use in drug delivery applications. *Carbohydr Polym* 157:185–195
53. Jarrahpour A, Doroodmand MM, Ebrahimi E (2012) The first report of [2+ 2] ketene–imine cycloaddition reactions (Staudinger) on carbon nanotubes. *Tetrahedron Lett* 53(23):2797–2801
54. Esmailpour M, Sardarian AR, Jarrahpour A, Ebrahimi E, Javidi J (2016) Synthesis and characterization of  $\beta$ -lactam functionalized superparamagnetic Fe<sub>3</sub>O<sub>4</sub>@SiO<sub>2</sub> nanoparticles as an approach for improvement of antibacterial activity of  $\beta$ -lactams. *RSC Adv* 6(49):43376–43387
55. Turos E, Reddy GSK, Greenhalgh K, Ramaraju P, Abeylath SC, Jang S, Dickey S, Lim DV (2007) Penicillin-bound polyacrylate nanoparticles: restoring the activity of  $\beta$ -lactam antibiotics against MRSA. *Bioorg Med Chem Lett* 17(12):3468–3472
56. Ebrahimi E, Jarrahpour A, Heidari N, Sinou V, Latour C, Brunel JM, Zolghadr AR, Turos E (2016) Synthesis and antimalarial activity of new nanocopolymer  $\beta$ -lactams and molecular docking study of their monomers. *Med Chem Res* 25(2):247–262
57. Bardajee GR, Pourjavadi A, Ghavami S, Soleyman R, Jafarpour F (2011) UV-prepared salep-based nanoporous hydrogel for controlled release of tetracycline hydrochloride in colon. *J Photochem Photobiol B* 102(3):232–240
58. Britton HTS, Robinson RA (1931) CXCVIII.—Universal buffer solutions and the dissociation constant of veronal. *J Chem Soc*: 1456–1462
59. Peppas LBH, R.S. (1990) *Absorbent Polymer Technology*. Elsevier, Amsterdam, The Netherlands
60. Ebrahimi E, Jarrahpour A (2014) Thionyl chloride (or oxalyl chloride) as an efficient acid activator for one-pot synthesis of [Beta]-lactams. *Iran J Sci Technol A* 38(A1):49
61. Karimi A, Wan Daud WMA (2017) Materials, preparation, and characterization of PVA/MMT nanocomposite hydrogels: a review. *Polym Compos* 38(6):1086–1102
62. Bortolin A, Aouada FA, Mattoso LH, Ribeiro C (2013) Nanocomposite PAAm/methyl cellulose/montmorillonite hydrogel: evidence of synergistic effects for the slow release of fertilizers. *J Agric Food Chem* 61(31):7431–7439
63. Chatterjee A, Ebina T, Onodera Y, Mizukami F (2004) Effect of exchangeable cation on the swelling property of 2: 1 dioctahedral smectite—a periodic first principle study. *J Chem Phys* 120(7): 3414–3424
64. Wang Y, He G, Li Z, Hua J, Wu M, Gong J, Zhang J, Li-tong B, Huang L (2018) Novel biological hydrogel: swelling behaviors study in salt solutions with different ionic valence number. *Polymers* 10(2):112
65. Buchholz FL, Peppas NA (1994) *Superabsorbent polymers: science and technology*. ACS Publications
66. Omidian H, Hashemi S, Sammes P, Meldrum I (1999) Modified acrylic-based superabsorbent polymers (dependence on particle size and salinity). *Polymer* 40(7):1753–1761
67. Zhang J, Yuan K, Wang Y-P, Zhang S-T, Zhang J (2007) Preparation and PH responsive behavior of poly(vinyl alcohol)—chitosan—poly(acrylic acid) full-IPN hydrogels. *J Bioact Compat Polym* 22(2):207–218
68. Dil NN, Sadeghi M (2018) Free radical synthesis of nanosilver/gelatin-poly(acrylic acid) nanocomposite hydrogels employed for antibacterial activity and removal of Cu(II) metal ions. *J Hazard Mater* 351:38–53

**Publisher's note** Springer Nature remains neutral with regard to jurisdictional claims in published maps and institutional affiliations.